Supplementary Information

Angelini *et al.*, Directed evolution of broadly crossreactive chemokine-blocking antibodies efficacious in arthritis

Supplementary Discussion

Potential mechanisms of SA138 and SA157* broad crossreactivity

Conformational changes and structural plasticity might enable different optimal geometries and the exploration of alternative energetically favorable interactions that adapt to the topology of diverse targets needed for broad crossreactivity[1-4]. These rearrangements could involve local side chains and loop reorientations as well as the global rearrangement of the entire backbone and scaffold (e.g. movements of V_L and V_H domains). Notably, the addition of stabilizing intermolecular disulfide bridges (ds) to the broadly crossreactive SA138 and SA157* molecules had adverse consequences on both expression and binding to ELR^+ CXC chemokines (**Supplementary Fig. 8**). We speculate that the presence of disulfide bond pairs in highly promiscuous antibodies could have imposed rigidity by restricting the geometry of the V_L-V_H dimer to non-optimal binding conformations. Indeed, single V_L and V_H domains of SA157* are stable only when produced separately and are able to bind the target when mixed equimolarly. Therefore, SA157* in particular may very well represent an extreme case of crossreactivity achieved though conformational flexibility. In contrast to the broadly crossreactive clones SA138 and SA157*, no decrease in binding affinity was observed when intermolecular disulfide bridges were added to two different locations of the more specific SA129. This is in line with previous studies reporting the acquisition of mutations that confer structural rigidity during the evolution of highly specific antibodies[2, 4, 5].

Binding promiscuity could also have been achieved through entropy-driven interactions[6]. Intriguingly, enrichment in proline residues has been observed for both highly crossreactive CK138 and CK157 molecules. Prolines are known to impose conformational constraints and

rigidity on protein loops leading to smaller losses of conformational entropy on binding and ultimately increased affinity[7]. Similar roles have been attributed to proline residues present on bNAbs and other naturally evolved crossreactive proteins[8]. We speculate that the presence of proline in the binding loops of our crossreactive antibodies might induce favorable conformations, thus facilitating binding of multiple structurally similar ELR^+ CXC chemokines through molecular mimicry mechanisms, a phenomena often refereed as "rigid adaptation"[9]. Co-evolution of both crossreactivity and binding affinity may require the combination of conformational flexibility and rigidity, with mutations inducing flexibility and promiscuity coexisting with and compensated by mutations that confer rigidity and increase binding affinity[10, 11].

Finally, we cannot exclude the possibility that broad crossreactivity may have been achieved through differential ligand positioning, a mechanism in which a single antibody recognizes different antigens by exploiting spatially distinct regions of its binding site[12]. However, while site-directed mutagenesis approaches are useful to map the epitopes that influence binding and specificity, more accurate measurements of energetic contributions to binding, including three-dimensional structures of crossreactive antibodies in complex with different ELR^+ CXC chemokines, will be required to fully understand the underlying molecular basis of binding promiscuity.

Supplementary Figures

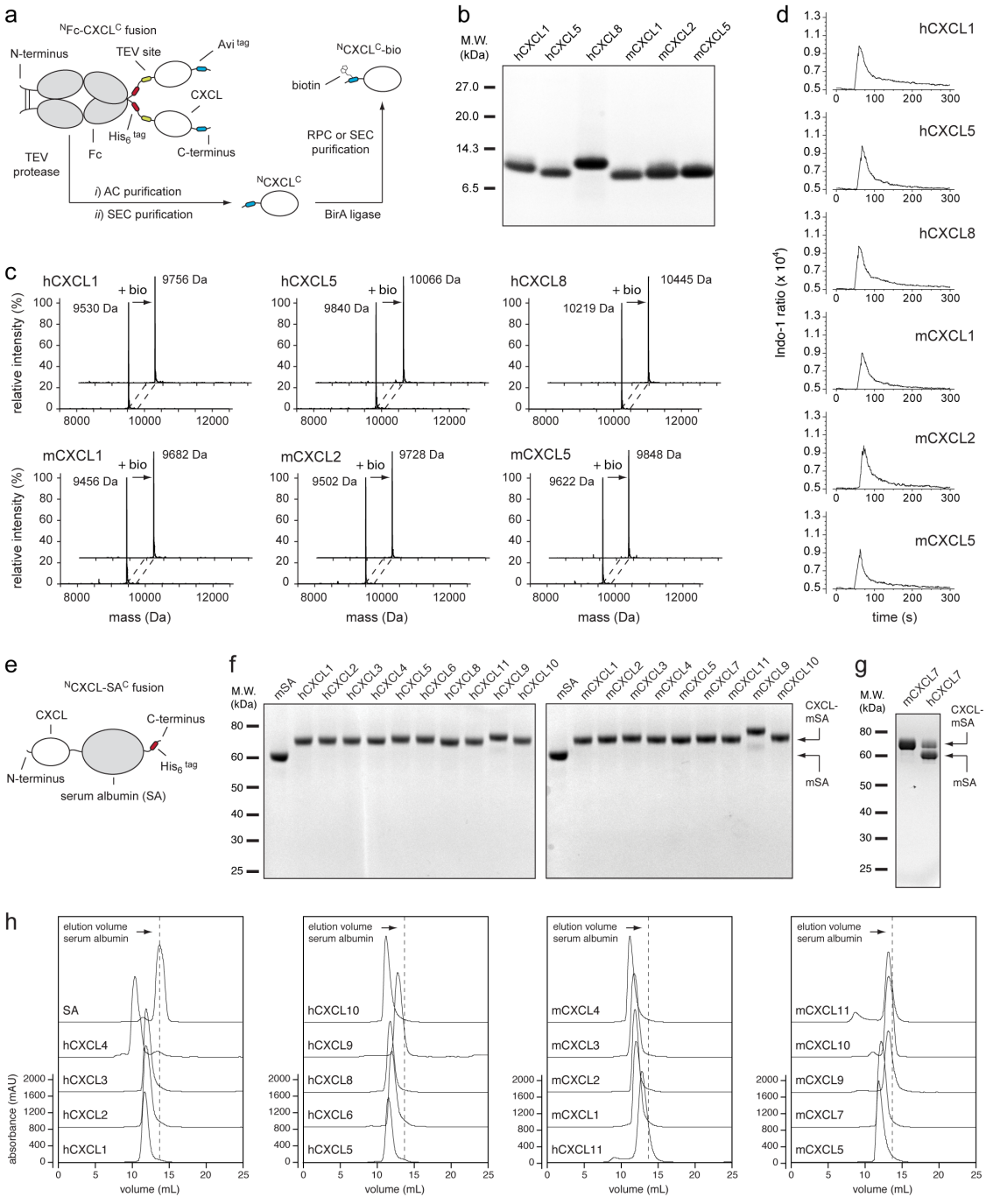

Supplementary Figure 1. Production and characterization of CXC chemokines. a) Schematic representation of the (*i*) Fc-ELR$^+$ CXC chemokine fusion protein constructs (Fc-CXCL) and (*ii*) purification scheme applied to obtain pure, active and biotinylated ELR$^+$ CXC

chemokines (CXCL-bio). The Fc domain derived from a murine IgG2 heavy-chain constant regions C_H2 and C_H3 is colored in grey, the hexa-histidine tag (His_6) in red, the Tobacco Etch Virus proteolytic cleavage site (TEV) in yellow, the ELR^+ CXC chemokine in white and the 15 amino acid peptide target sequence AviTag for biotin ligase BirA in blue. Superscript N and C letters indicate the N- and C-terminus respectively; **b**) Comassie blue stained SDS-PAGE of purified and biotinylated ELR^+ CXC chemokines. M.W., molecular-weight size markers; **c**) Mass spectra of human (hCXCL1, hCXCL5 and hCXCL8) and murine (mCXCL1, mCXCL2 and mCXCL5) ELR^+ CXC chemokines before and after enzymatic biotinylation. All the masses are shifted by 226 Da, which corresponds to the mass change upon reaction with one biotin molecule; **d**) Tracing representing the ratiometric measurement of calcium using fluorescent indicator Indo-1 AM. Results are expressed as Indo-1 ratio against time (seconds). Purified human and murine derived neutrophils loaded with Indo-1 were stimulated with 10 nM of biotinylated ELR^+ CXC chemokines. Baseline fluorescence was recorded for 60 seconds before the addition of biotinylated ELR^+ CXC chemokines and ratio fluorescence was measured for an additional 240 seconds; **e**) Schematic representation of the CXC chemokine expressed as N-terminal fusion to mouse serum albumin (CXCL-SA). Mouse serum albumin (mSA) is colored in grey, the ELR^+ CXC chemokine in white and the hexa-histidine tag (His_6) in red; **f**) Comassie blue stained SDS-PAGE of purified human and murine CXCL-SA fusion proteins; **g**) Comassie blue stained SDS-PAGE of purified mouse serum albumin fusion murine mCXCL7 and human hCXCL7. While murine mCXCL7 fused to SA remained stable, the orthologous human hCXCL7 underwent degradation thus explaining its ability to bind antibodies when displayed on the surface on yeast but not when expressed as soluble SA fusion; **h**) Analytical size-exclusion chromatography of the purified CXCL-SA fusion proteins. All the proteins showed a high degree of purity and most of them were eluted at an elution volume (V_e) of about 12-13 mL that corresponds to proteins with an apparent molecular weight of 150 kDa, which agree with the dimeric state of CXCL-SA fusions. Highly oligomeric proteins hCXCL4 and hCXCL10 fusions are eluted at a V_e of about 10-11 mL that corresponds to a protein with a apparent molecular weight of 300 kDa, which agree with the tetrameric state of the fusions. mSA alone is eluted at a V_e of about 13.5 mL, which corresponds to a protein with an apparent molecular weight of 66 kDa.

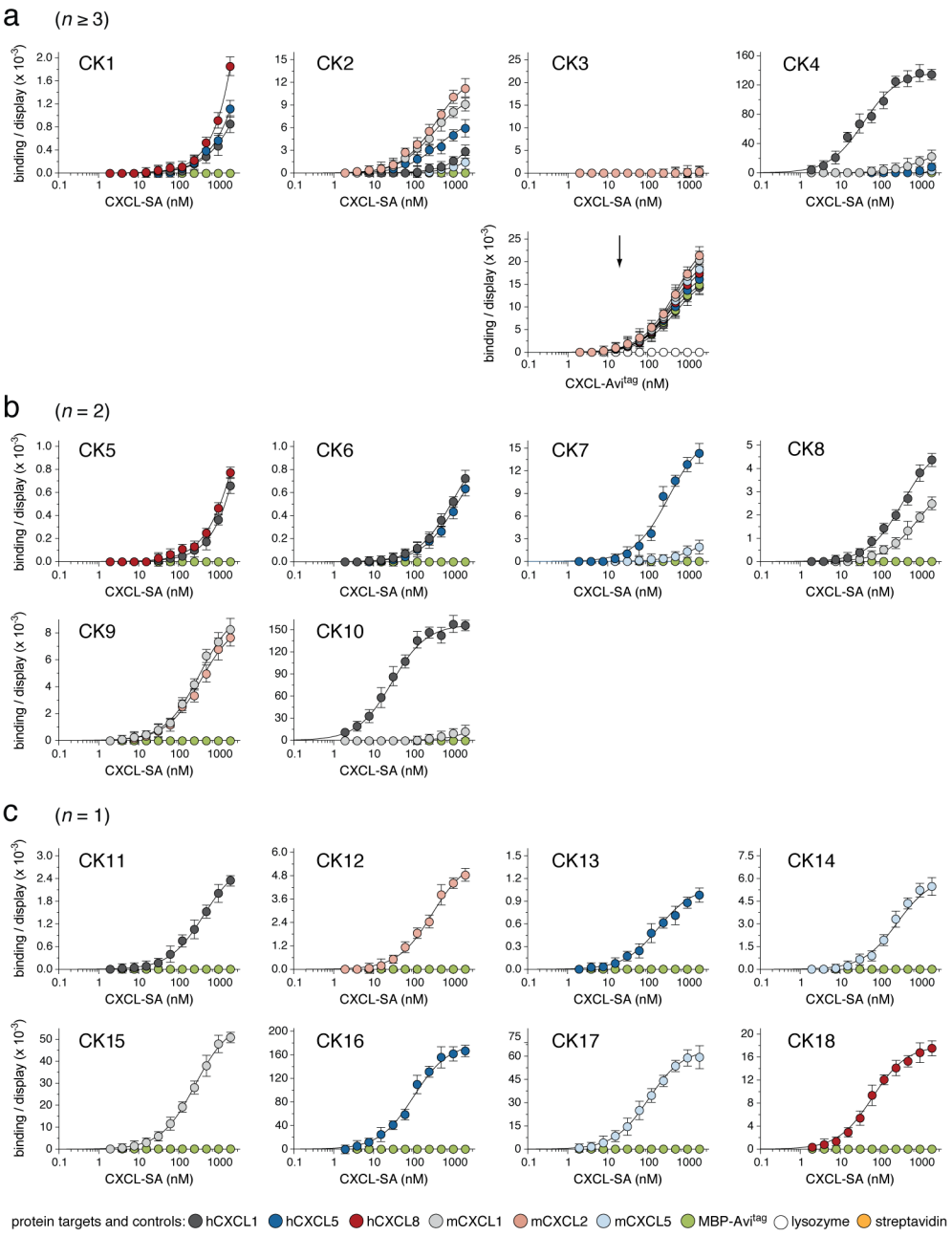

Supplementary Figure 2. **Binding titrations of selected antibody clones. a**) Binding titration of yeast-displayed antibody clones CK1, CK2, CK3 and CK4 that crossreact with at least three ELR$^+$ CXC chemokines ($n \geq 3$). Clone CK3 does not bind the ELR$^+$ CXC chemokine-SA fusion proteins (CXCL-SA) lacking the C-terminus biotinylated AviTag sequence; **b**) Binding titrations of yeast displayed antibody clones CK5, CK6, CK7, CK8, CK9 and CK10 that recognize two ELR$^+$ CXC chemokines ($n = 2$); **c**) Binding titrations of yeast displayed antibody clones CK11,

CK12, CK13, CK14, CK15, CK16, CK17 and CK18 that bind only one ELR^+ CXC chemokine (n = 1). Binding of selected yeast displayed antibody clones against soluble ELR^+ CXC chemokines were assessed by flow cytometry-based assay. The obtained fluorescence binding median intensities were normalized to the display median fluorescence intensities. ELR^+ CXC chemokines and the corresponding binding/display values (y-axis) are indicated as differently colored filled circles and represent the means of at least three independent experiments plotted against varying concentrations of soluble CXCL-SA fusions (2 - 2000 nM; x-axis). Control proteins: biotinylated maltose binding protein bearing the AviTag (MBP-AviTag), biotinylated lysozyme and fluorescently labeled streptavidin are colored in green, white and orange, respectively.

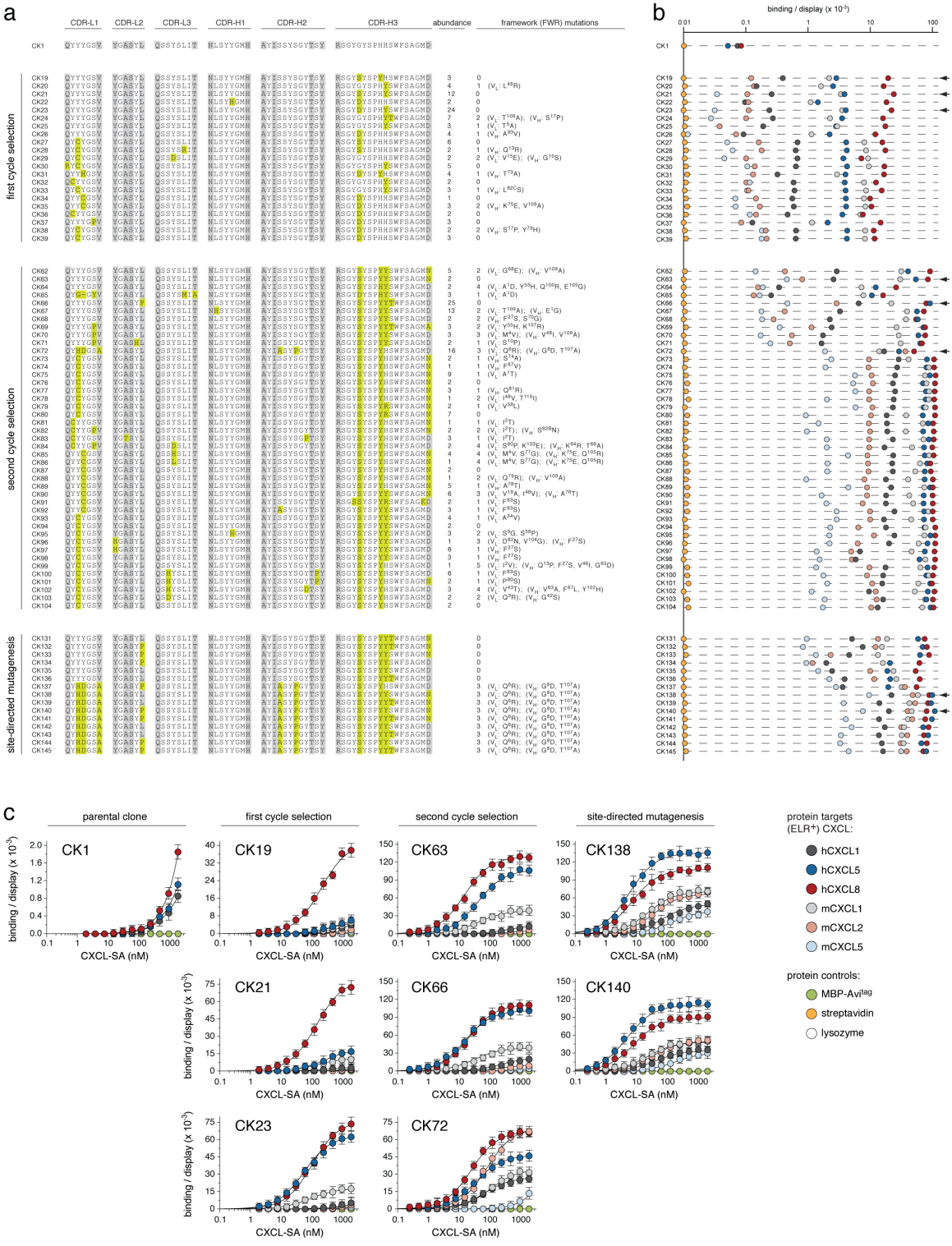

Supplementary Figure 3. Molecular co-evolution of CK1 affinity and crossreactivity. a) Amino acid sequence of clones isolated from two independent iterative processes of selection

(first and second cycle), each including the generation of random yeast-display antibody libraries and six cycles of flow cytometry sorting, followed by a third round of site-directed mutagenesis. The CDRs regions of light (VL: CDR-L1, CDR-L2 and CDR-L3) and heavy (VH: CDR-H1, CDR-H2 and CDR-H3) chains are shown. Mutated residues within the CDRs are shaded light green. Non-diversified positions present within the CDRs are shaded light gray. Abundance indicates the number of times an individual clone has been observed. The total number and the location of the mutations accumulated within the FWRs are indicated; **b**) Fluorescence binding signals of yeast displayed CK1 derived clones against soluble ELR^+ CXC chemokine were assessed by a flow cytometry-based assay. Binding intensities have been measured using single concentration of soluble biotinylated chemokine (50 nM) and obtained median values were normalized to the display median fluorescence intensities; **c**) Binding titration of the CK1 and its best derived clones isolated from each iterative process of selection. Binding of molecular co-evolved yeast displayed antibody clones against soluble ELR^+ CXC chemokines were assessed by flow cytometry-based assay. The obtained fluorescence binding median values were normalized to the display median fluorescence intensities. ELR^+ CXC chemokines and the corresponding binding/display values (*y*-axis) are indicated as differently colored filled circles and represent the means of at least three independent experiments plotted against varying concentrations of soluble CXCL-SA fusions (0.2 - 2000 nM; *x*-axis). Control proteins: biotinylated maltose binding protein bearing the AviTag (MBP-AviTag), biotinylated lysozyme and fluorescently labeled streptavidin are colored in green, white and orange, respectively.

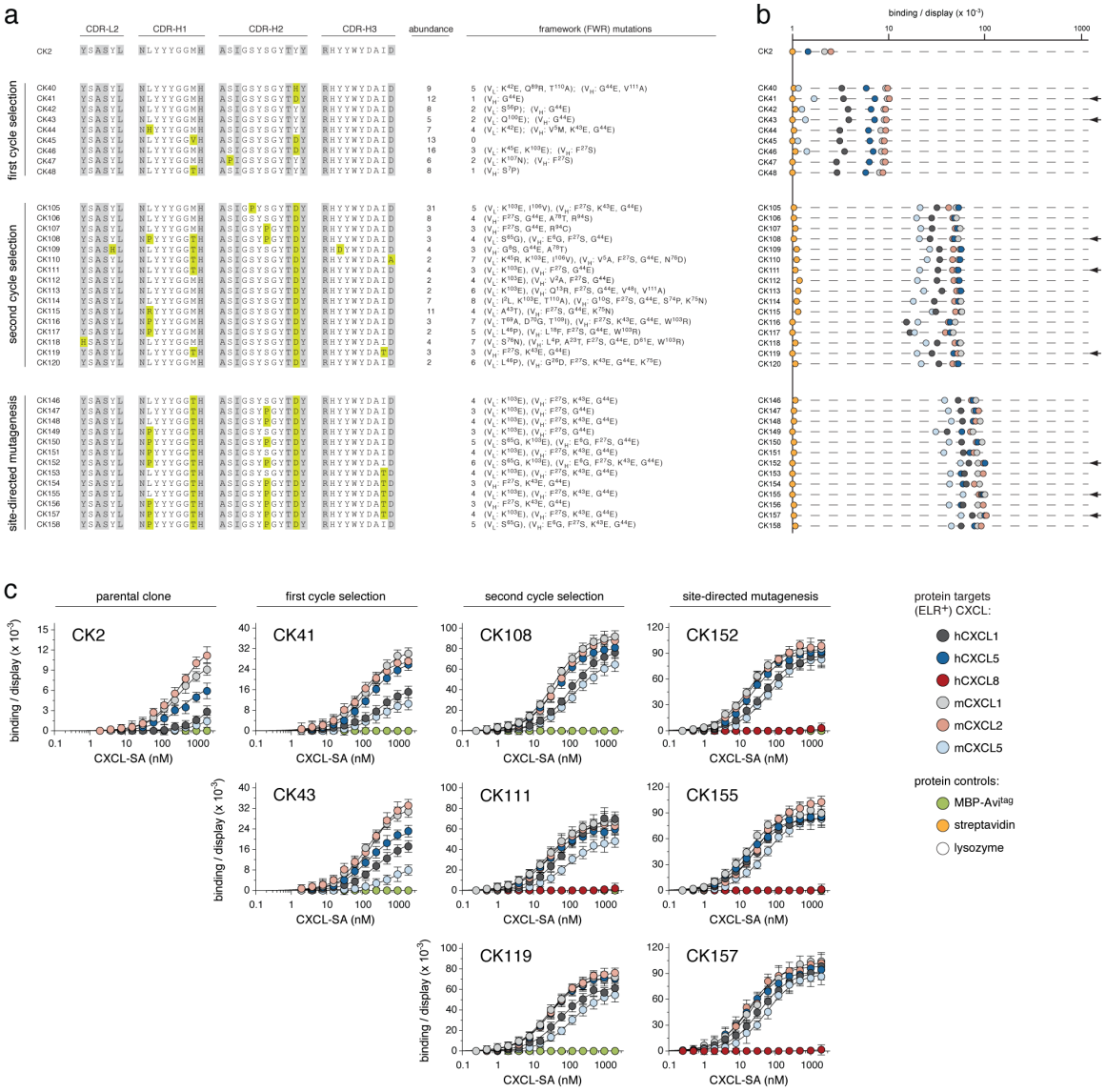

Supplementary Figure 4. Molecular co-evolution of CK2 affinity and crossreactivity. a) Amino acid sequence of clones isolated from two independent iterative processes of selection (first and second cycle), each including the generation of random yeast-display antibody libraries and five cycles of flow cytometry sorting, followed by a third round of site-directed mutagenesis. The CDRs regions of light (VL: CDR-L2) and heavy (VH: CDR-H1, CDR-H2 and CDR-H3) chains are shown. Mutated residues within the CDRs are shaded light green. Non-diversified positions present within the CDRs are shaded light gray. Abundance indicates the number of times an individual clone has been observed. The total number and the location of the mutations accumulated within the FWRs are indicated; **b**) Fluorescence binding signals of yeast displayed

CK2 derived clones against soluble ELR^+ CXC chemokine were assessed by a flow cytometry-based assay. Binding intensities have been measured using single concentration of soluble biotinylated chemokine (50 nM) and obtained median values were normalized to the display median fluorescence intensities; **c**) Binding titration of the CK2 and its best derived clones isolated from the each iterative process of selection. Binding of molecular co-evolved yeast displayed antibody clones against soluble ELR^+ CXC chemokines were assessed by flow cytometry-based assay. The obtained fluorescence binding median values were normalized to the display median fluorescence intensities. ELR^+ CXC chemokines and the corresponding binding/display values (*y*-axis) are indicated as differently colored filled circles and represent the means of at least three independent experiments plotted against varying concentrations of soluble CXCL-SA fusions (0.2 - 2000 nM; *x*-axis). Control proteins: biotinylated maltose binding protein bearing the AviTag (MBP-AviTag), biotinylated lysozyme and fluorescently labeled streptavidin are colored in green, white and orange, respectively.

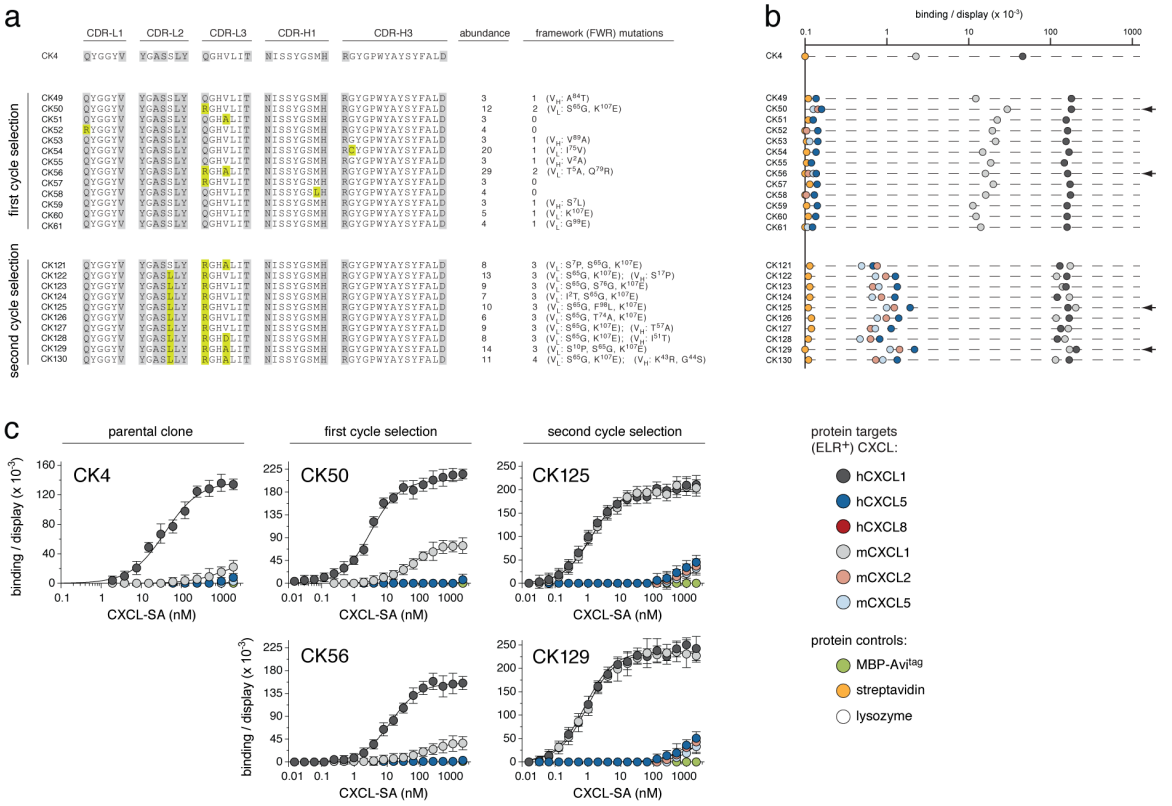

Supplementary Figure 5. Molecular co-evolution of CK4 affinity and crossreactivity. a) Amino acid sequence of clones isolated from two independent iterative processes of selection (first and second cycle), each including the generation of random yeast-display antibody libraries and five cycles of flow cytometry sorting. The CDRs regions of light (VL: CDR-L1, CDR-L2 and CDR-L3) and heavy (VH: CDR-H1 and CDR-H3) chains are shown. Mutated residues within the CDRs are shaded light green. Non-diversified positions present within the CDRs are shaded light gray. Abundance indicates the number of times an individual clone has been observed. The total number and the location of the mutations accumulated within the FWRs are indicated; **b**) Fluorescence binding signals of yeast displayed CK4 derived clones against soluble ELR$^+$ CXC chemokine were assessed by a flow cytometry-based assay. Binding intensities have been measured using single concentration of soluble biotinylated chemokine (50 nM) and obtained median values were normalized to the display median fluorescence intensities; **c**) Binding titration of the CK4 and its best derived clones isolated from the each iterative process of selection. Binding of molecular co-evolved yeast displayed antibody clones against soluble ELR$^+$ CXC chemokines were assessed by flow cytometry-based assay. The obtained

fluorescence binding median values were normalized to the display median fluorescence intensities. ELR^+ CXC chemokines and the corresponding binding/display values (*y*-axis) are indicated as differently colored filled circles and represent the means of at least three independent experiments plotted against varying concentrations of soluble CXCL-SA fusions (0.02 - 2000 nM; *x*-axis). Control proteins: biotinylated maltose binding protein bearing the AviTag (MBP-AviTag), biotinylated lysozyme and fluorescently labeled streptavidin are colored in green, white and orange, respectively.

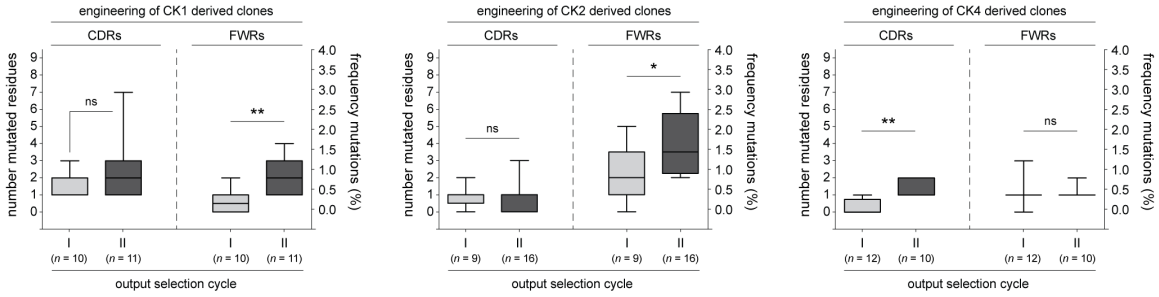

Supplementary Figure 6. Frequency and distribution of mutations. Box and whiskers graph comparing the value of total number (left *y*-axis) and frequencies (right *y*-axis) of accumulated mutations within CDRs (plot's left side) and FWRs (plot's right side) regions of both V_L and V_H domains of CK1 (left), CK2 (middle) and CK4 (right) derived clones selected after the first (I) and second (II) cycle of selection. "*n*" indicates samples size. The middle line within each box represents the median, and the lower and upper boundaries of the box indicate the 25th (Q1) and 75th (Q3) percentiles. Whiskers represent the 1.5 × interquartile range (IQR = Q3 – Q1) extending beyond box. Statistical comparisons were made between each group using one-way analysis of variance (ANOVA), followed by Tukey's test to calculate *P* values: **P* < 0.05, ** *P* < 0.01, *** *P* < 0.001; **** *P* < 0.0001. ns: non-significant.

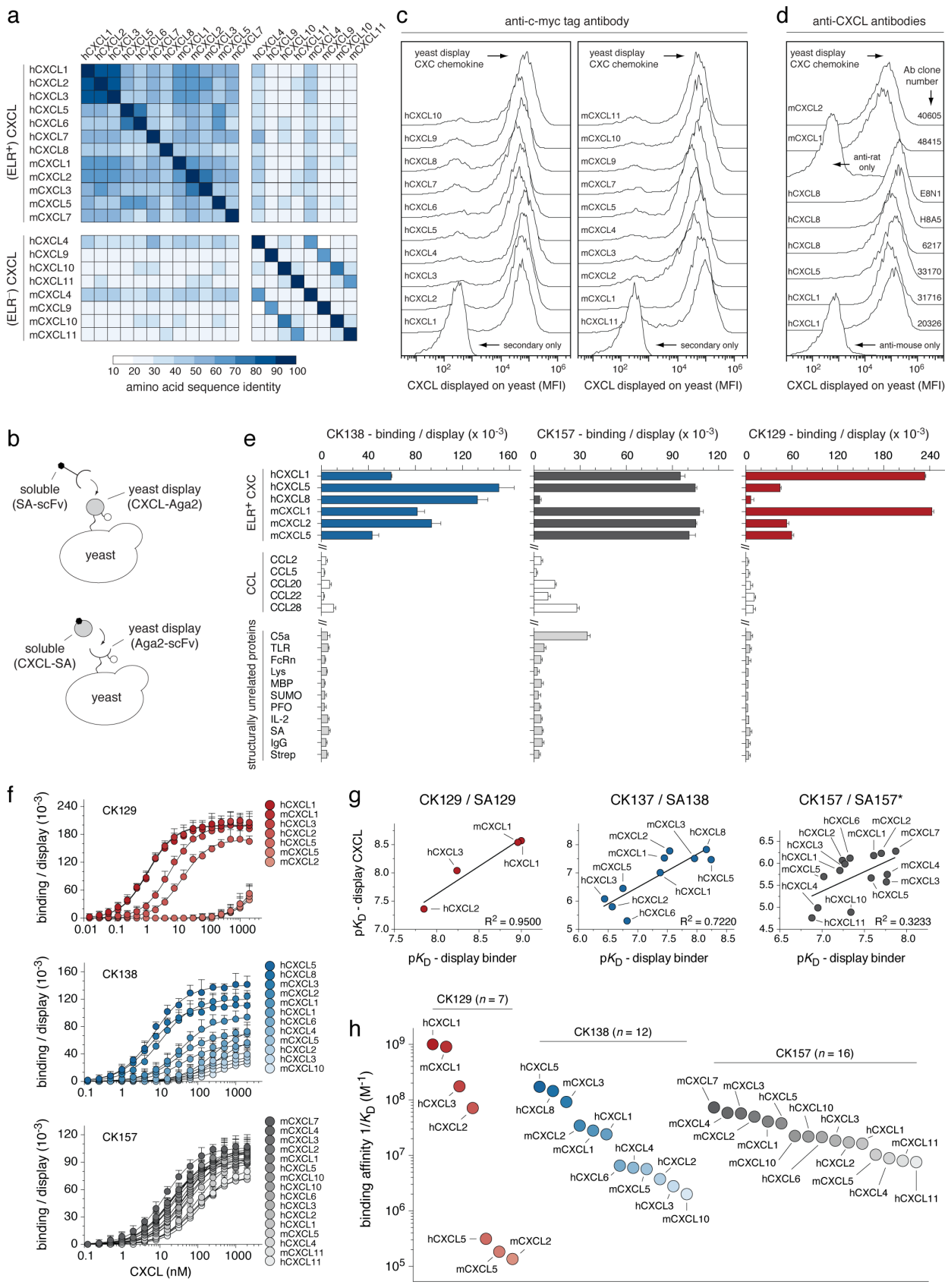
a
(ELR+) CXCL
(ELR−) CXCL
amino acid sequence identity
b
soluble (SA-scFv)
yeast display (CXCL-Aga2)
yeast
soluble (CXCL-SA)
yeast display (Aga2-scFv)
yeast
c
anti-c-myc tag antibody
yeast display CXC chemokine
secondary only
CXCL displayed on yeast (MFI)
d
anti-CXCL antibodies
Ab clone number
anti-rat only
anti-mouse only
e
CK138 - binding / display (x 10-3)
CK157 - binding / display (x 10-3)
CK129 - binding / display (x 10-3)
ELR+ CXC
CCL
structurally unrelated proteins
f
CK129
CK138
CK157
binding / display (10-3)
CXCL (nM)
g
CK129 / SA129
CK137 / SA138
CK157 / SA157*
pKD - display CXCL
pKD - display binder
R2 = 0.9500
R2 = 0.7220
R2 = 0.3233
h
CK129 (n = 7)
CK138 (n = 12)
CK157 (n = 16)
binding affinity 1/KD (M-1)

Supplementary Figure 7. Crossreactivity of engineered antibodies toward multiple CXC chemokines. a) Heat map displaying the sequence identity among multiple human and murine CXC chemokines. The color of each element in the heat map indicates the percent of sequence identity, ranging from 10% (white) to 100% (dark blue); **b**) Symmetrical yeast display arrangements: *i*) soluble SA-scFv toward CXC chemokines displayed on the surface of yeast cells (top) and *ii*) soluble CXCL-SA fusions against yeast-displayed antibodies (gray; bottom); **c**) Flow cytometry analysis of the expression of human and murine CXC chemokines displayed on the surface of yeast cells as N-terminal fusion to Aga2p protein after staining with anti-c-myc antibody; **d**) Proper folding of three human and two murine ELR^+ CXC chemokines displayed on the surface of yeast cells was confirmed by staining with commercial anti-chemokine antibodies (Ab; **Supplementary Table 13**); **e**) Columns graph reporting the fluorescence binding intensities of yeast-displayed CK138 (blue), CK157 (dark gray) and CK129 (red) against six soluble CXCL-SA fusions, five structurally related CCL chemokines (white; **Supplementary Table 13**), and eleven structurally unrelated proteins (light gray; C5a: murine complement component C5a; TLR: toll-like receptor; FcRn: neonatal Fc receptor; Lys: lysozyme; MBP: maltose binding protein; SUMO: small ubiquitin-like modifier protein; PFO: perfringolysin O toxin; IL-2: interleukin-2; SA: serum albumin; IgG: immunoglobulin; Strep: streptavidin). Fluorescence binding signals were assessed by a flow cytometry-based assay using single concentrations (2 μM) of soluble proteins. Obtained median values were normalized to the display median fluorescence intensities of each single yeast surface displayed partner (binding/display). Normalized values (*y*-axis) represent the means ± s.e.m. (bars) of at least three independent experiments; **f**) Binding isotherms of yeast-displayed CK129 (red), CK138 (blue) and CK157 (gray) antibodies to soluble human and murine CXCL-SA fusions (0.01 - 2000 nM). Equilibrium binding affinities (K_D) were determined only for pairs exhibiting binding signals against high concentrations of soluble CXCL-SA fusions. Obtained binding median values were normalized to the display median fluorescence intensities of each single yeast surface displayed partner (binding/display). CXC chemokines and the corresponding binding/display values (*y*-axis) are indicated as differently colored filled circles and represent the means (dots) ± s.e.m. (bars) of at least three independent experiments plotted against varying concentrations of soluble serum albumin-antibody fusions (*x*-axis); **g**) Scatter plot showing the correlation between the experimental pK_D values determined using the two complementary cell display arrangements:

soluble CXCL-SA fusions against yeast-displayed antibodies (*x*-axis, "pK_D – display binder scFv") and soluble SA129, SA138 and SA157* fusions against CXC chemokines displayed on the surface of yeast cells (*y*-axis, "pK_D – display CXCL"). R^2 indicates the coefficient of determination; **h**) Plot of the binding affinities of yeast-displayed antibodies CK129 (red), CK138 (blue) and CK157 (gray) to soluble human and murine CXCL-SA fusions. The measured K_D values are indicated as differently colored filled circles and presented as inverted of equilibrium binding constants ($1/K_D$; M^{-1}). CXC chemokines are gradient colored ranging from dark (high affinity) to light (low affinity) red (SA129), blue (SA138) and gray (SA157) colors.

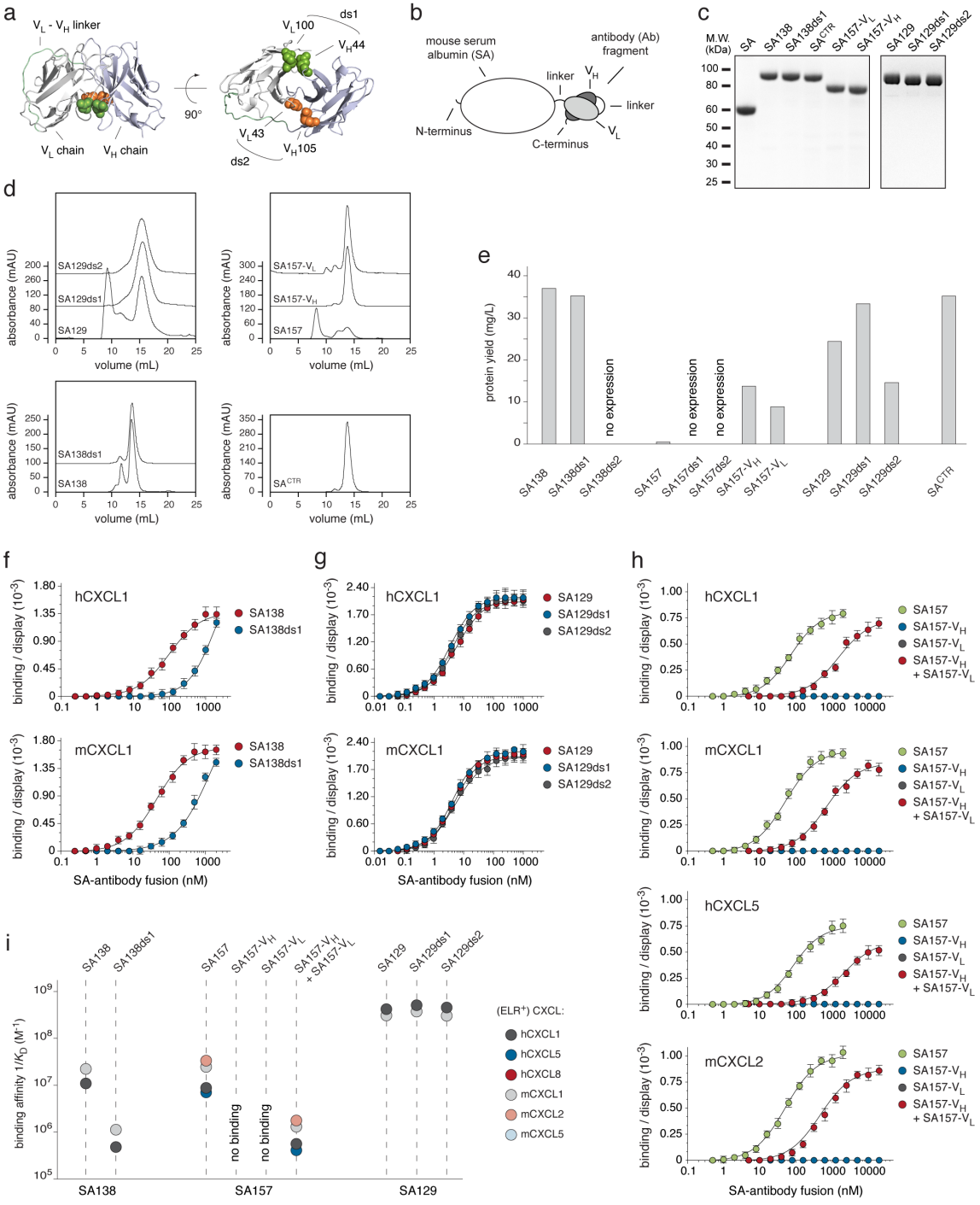

Supplementary Figure 8. Production and characterization of serum albumin-antibody fusions. a) Variable light V_L (gray) and heavy V_H (light blue) chains of a single-chain variable synthetic antibody fragment (PDB ID: 2KH2)[13], separated by a flexible linker are represented as ribbons. The structure is shown in two orientations (90° rotation) to allow the visualization of the

two most favorable locations selected for the introduction of pairs of cysteine residues into each single antibody fragment: ds1: V_L100 and V_H44 (green spheres); ds2: V_L43 and V_H105 (orange spheres; Kabat numbering system)[14-16]. ds, intermolecular disulfide bond connecting the V_L and V_H variable domains. Models were rendered using PyMOL (PyMOL Molecular Graphics System, Version 1.8 Schrödinger, LLC); **b**) Schematic representation of the antibody single-chain variable fragment fused the C-terminus of mouse serum albumin to generate SA129, SA138 and control SA^{CTR} fusion proteins. SA^{CTR} is used as control ("CTR") and it encodes for SA fused to sm3E, an antibody fragment targeting the carcinoembryonic antigen (CEA), a protein that does not exist in mice[17]; **c**) Comassie blue stained SDS-PAGE of purified serum albumin-antibody clones used for *in vitro* and *in vivo* studies. From the left to the right: serum albumin (SA), wild-type SA138, disulfide-stabilized SA138ds1, SA^{CTR} fusion, light and heavy chain of SA157 fused to the C-terminus of mouse serum albumin (SA157-V_L and SA157-V_H); wild-type SA129, disulfide-stabilized SA129ds1 and SA129ds2. M.W., molecular-weight size markers; **d**) Analytical size-exclusion chromatography of the purified serum albumin-antibody fusion proteins. Top left, SA129ds1 and SA129ds2 showed a high degree of purity and increased percent of monomeric forms compared to the wild-type SA129. Bottom left, SA138ds1 showed a high degree of purity and increased percent of monomeric forms compared to the wild-type SA138. Top right, single V_L and V_H chain of CK157 antibody clone separately fused to the C-terminus of mouse serum albumin (SA157-V_L and SA157-V_H) showed a high degree of purity and increased percent of monomeric forms compared to the wild-type SA157. Bottom right, analytical size-exclusion chromatography of the purified SA^{CTR} fusion; **e**) Columns graph reporting the final protein yield (mg L^{-1}) of the purified SA-antibody fusions from 1 L of HEK293 mammalian cell culture. The final yield of wild-type SA157 was extremely low (< 0.5 mg L^{-1}) while no expression was detected for disulfide-stabilized SA138ds2, SA157ds1 and SA157ds2; **f**) Binding titration of SA138 (red circle) and SA138ds1 (blue circle) against yeast-displayed hCXCL1 (top) and mCXCL1 (bottom) chemokines; **g**) Binding titration of SA129 (red circle), SA129ds1 (blue circle) and SA129ds2 (gray circle) against yeast-displayed hCXCL1 (top) and mCXCL1 (bottom) chemokines; **h**) Binding titration of SA157 (green circle), SA157-V_H (blue circle), SA157-V_L (gray circle) and equimolarly combined CK157-V_H + CK157-V_L fusions (SA157*, red circle) against yeast-displayed hCXCL1 (top), mCXCL1, hCXCL5 and mCXCL2 (bottom) chemokines. Binding of yeast displayed ELR^+ CXC chemokines against

soluble SA129, SA138 and SA157 were assessed by flow cytometry-based assay. The obtained fluorescence binding median values were normalized to the display median fluorescence intensities. ELR^+ CXC chemokines and the corresponding binding/display values (*y*-axis) are indicated as differently colored filled circles and represent the means of at least three independent experiments plotted against varying concentrations of soluble serum albumin-antibody fusions (0.03 - 30000 nM; *x*-axis); **i**) Plot of the binding affinities of purified SA-antibody fusion proteins as determined from titration curves in panel **f**, **g** and **h**. ELR^+ CXC chemokines and the corresponding binding affinity values are reported as differently colored filled circles and indicate the means of at least three independent experiments. Data are presented as inverted of equilibrium binding constants ($1/K_D$; M^{-1}).

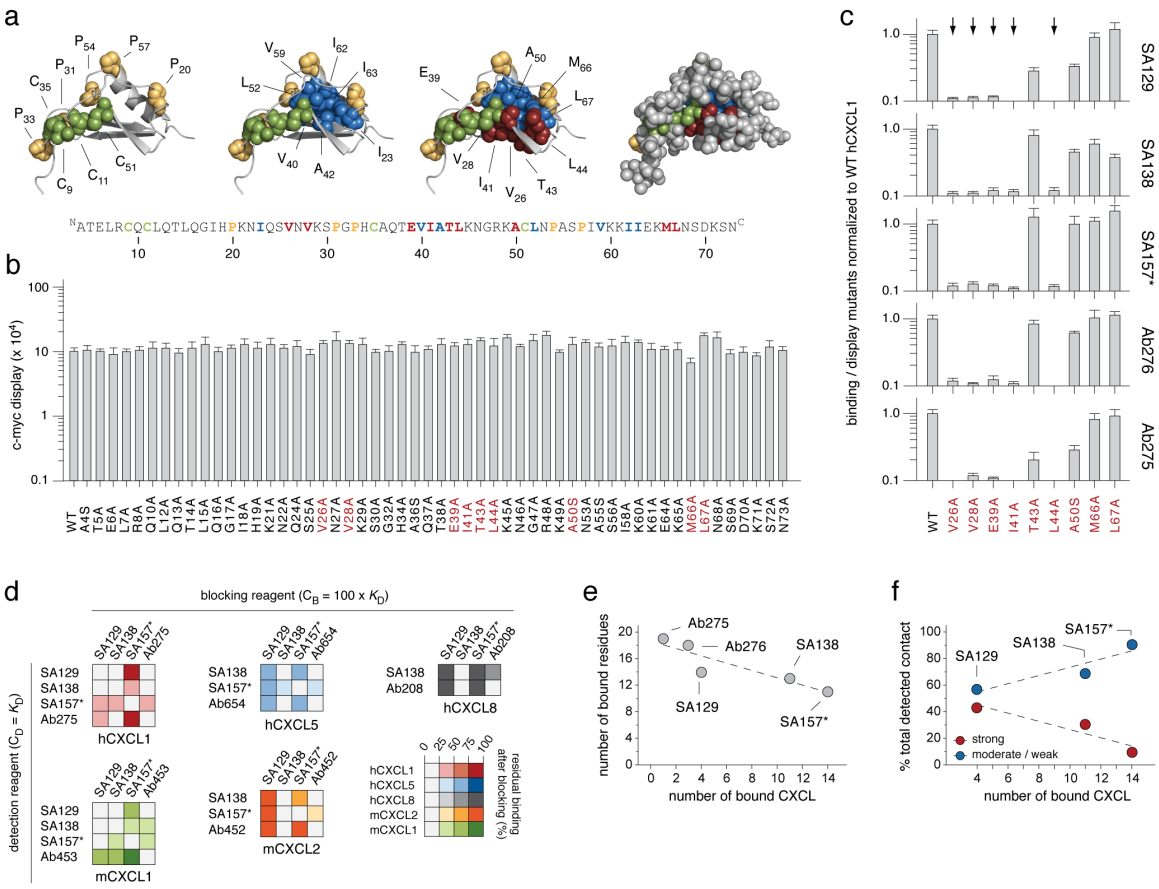

Supplementary Figure 9. Epitope mapping of crossreactive antibodies. a) The commonly bound human ELR$^+$ CXC chemokine hCXCL1 was selected for alanine scanning. The amino acid sequence and tridimensional structure of hCXCL1 (PDB ID: 1MGS[18]) represented as light gray ribbons are shown. Proline residues (P20, P31, P33, P54 and P57 shown as yellow spheres), cysteine residues (C9, C11, C35 and C52 shown as green spheres) and structurally buried hydrophobic amino acids (I23, V40, A42, L52, V59, I62 and I63 shown as blue spheres) that are crucial for overall folding and stability of the chemokine were left unaltered. Amino acids V26, V28, E39, I41, T43, L44, A50, M66 and L67 for which the relative solvent exposure and degree of burial in the structure is ambiguous are shown as dark red spheres and still mutated to alanine. The remaining forty-five solvent exposed residues that have been mutated to alanine are shown as light gray spheres. Solvent accessibility of amino acid residues of human hCXCL1 was determined by using both ASAView[19] and PyMOL (PyMOL Molecular Graphics System, Version 1.8 Schrödinger, LLC) tools; **b**) Columns graph reporting the level of expression of each distinct hCXCL1 alanine mutant (*x*-axis) displayed on the surface of yeast cell. Fluorescence

binding intensities have been determined by flow cytometry (anti-c-myc antibody). The determined display values represent the mean ± s.e.m. (bars) of three independent experiments; **c**) Columns graph reporting the fluorescence binding intensities of yeast-displayed V26, V28, E39, I41, T43, L44, A50, M66 and L67 alanine-mutants and wild-type hCXCL1 against engineered promiscuous serum albumin-antibody fusions SA129, SA138, SA157* and commercial neutralizing monoclonal antibodies Ab276 and Ab275. Fluorescence binding intensities were assessed by a flow cytometry-based assay using concentrations of soluble antibodies that are equals to their K_D values. The obtained fluorescence binding median values were normalized to the display median fluorescence intensities of each single hCXCL1 alanine mutant (binding/display) and further normalized to the value measured for the wild-type hCXCL1. Normalized values (*y*-axis) represent the means ± s.e.m. (bars) of at least three independent experiments. Five hCXCL1 mutants V26, V28, E39, I41, and L44 that exhibited an intense loss of binding upon incubation with all antibodies have been removed while alanine-mutants T43, A50, M66 and L67 have been further characterized; **d**) Competitive binding assay of soluble SA129, SA138, SA157* fusions and neutralizing antibodies (Ab) for binding to hCXCL1 (red), hCXCL5 (blue), hCXCL8 (gray), mCXCL1 (green) and mCXCL2 (orange) chemokine displayed on the surface of yeast. Yeast cells displaying the chemokines were pre-incubated with concentration of soluble un-biotinylated antibodies ("blocking reagents"; C_B) that were equals to 100-times their K_D values followed by addition of soluble biotinylated antibodies ("detection reagents"; C_D) at concentrations that were equals to their K_D values. Binding was assessed by flow cytometry-based assay using fluorescently labeled streptavidin. The determined residual fluorescence binding levels after blocking are indicated in percentage (%) and represent the mean values of three independent experiments; **e**) Number of interacting residues plotted against the number of bound CXC chemokines ligands (CXCL); **f**) The percent of strong (red) and combined weak and moderate interactions (blue) of each selected protein binders (CK129 CK138 and CK157) are plotted against the number of bound CXC chemokines.

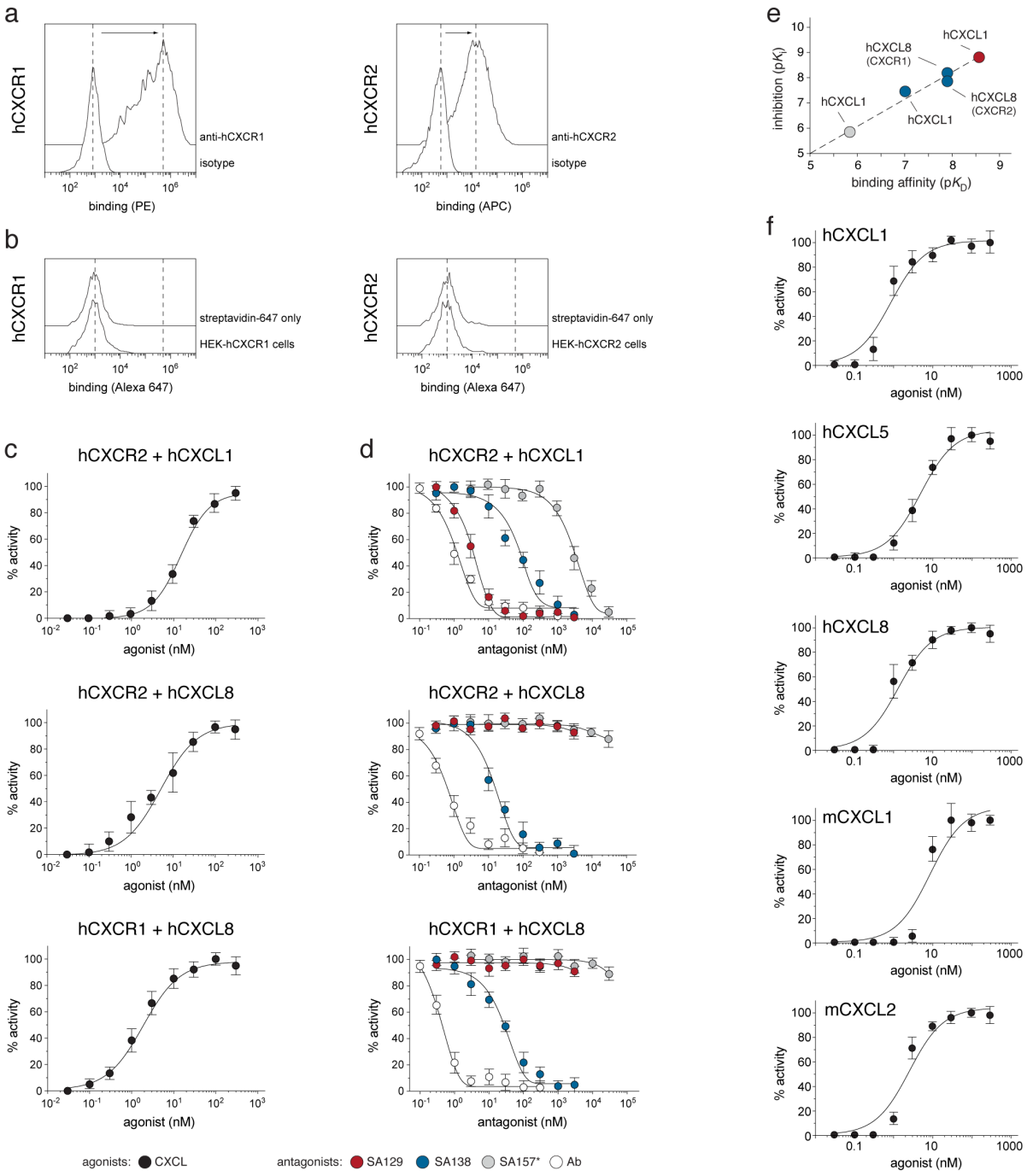

Supplementary Figure 10. Inhibition of receptor binding and activation. a) Histograms representing the flow cytometry analysis of surface expression of human CXCR1 (left) and CXCR2 (right) receptors in HEK cells after staining with PE anti-CXCR1 (clone 8F1) and APC anti-CXCR2 (clone 5E8) antibodies, respectively; **b**) Histograms representing the flow cytometry analysis of potential binding of secondary reagents only to HEK cells expressing

human CXCR1 and CXCR2 receptors in absence of biotinylated ELR^+ CXC chemokines; **c**) Dose-response titration curves dependent ELR^+ CXC chemokine binding using flow cytometry-based assay. Titration curves were obtained using increasing concentrations of biotinylated human hCXCL1 and hCXCL8 (0.03 – 300 nM) to human CXCR1 and CXCR2 and the EC_{50} determined; **d**) Competitive binding of biotinylated human hCXCL1 and hCXCL8 to human CXCR1 and CXCR2 in the presence of varying concentrations of SA129 (0.3 – 3000 nM, red), SA138 (0.3 – 3000 nM, blue), SA157* (0.003 – 30 μM, dark gray) fusions and commercial neutralizing anti-hCXCL1 and anti-hCXCL8 (0.1 – 300 nM) antibodies (Ab, light gray). Flow cytometry-based assay was performed using concentrations of agonist biotinylated human hCXCL1 and hCXCL8 that are equals to their EC_{50} values. Measured median fluorescence intensities were normalized to the maximal response obtained in the absence of antagonist and expressed as % of activity. Data represent the mean (dots) ± s.e.m. (bars) of three independent experiments; **e**) Plot displaying pK_i versus pK_D of SA129 (red), SA138 (blue), and SA157* (gray) fusions; **f**) Dose-response titration curves dependent ELR^+ CXC chemokine binding using ratiometric measurement of calcium in the presence of fluorescent indicator Indo-1 AM. Titration curves were obtained using purified human and murine derived neutrophils loaded with Indo-1 AM that have been stimulated with increasing concentrations of human hCXCL1, hCXCL5, hCXCL8 and murine mCXCL1 and mCXCL2 agonists (0.03 – 300 nM). The obtained values were normalized to the maximal response acquired, expressed as % of activity and the EC_{50} values determined. Data represent the mean (dots) ± s.e.m. (bars) of three independent experiments.

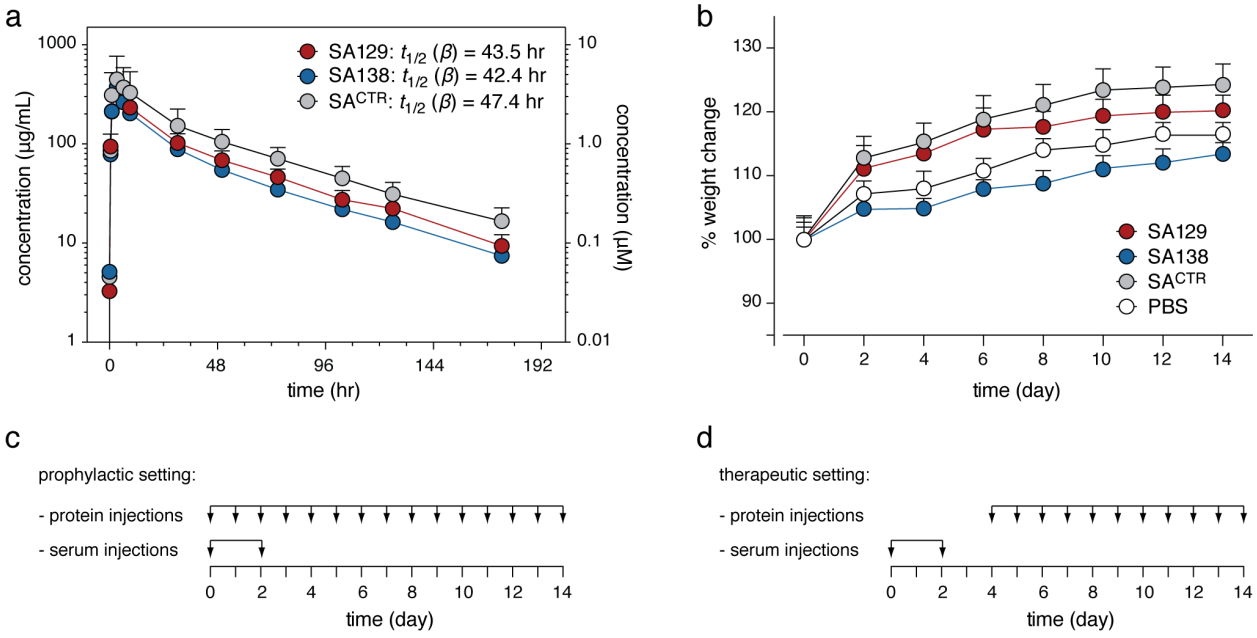

Supplementary Figure 11. Pharmacokinetic of serum albumin-antibody fusions. a) Pharmacokinetic profile of serum albumin-antibody fusions SA129 (red), SA138 (blue) and control SA^{CTR} (light gray) in C57BL/6 mice. A single dose (1 mg per mouse) of Alexa Fluor 647-labeled serum albumin-antibody fusions (2 mg mL^{-1}) were injected intraperitoneally (i.p.). Blood samples were collected at various time points (immediately after injection and at 0.5, 1, 2, 3, 5, 8, 24, 48, 72, 96, 120, and 168 hours post injection) and the concentration of fusion proteins determined by measuring the fluorescent intensity on a Typhoon imager[20]. The indicated data represent the mean (dots) ± s.e.m. (bars) of three mice per group (n = 3). The calculated $t_{1/2}$ (β) half-lives are reported for each serum albumin-antibody fusion: 42.4 hrs for SA138, 43.5 hrs for SA129 and 47.4 hrs for SA^{CTR}. The determined protein fusion concentration is reported in µg mL^{-1} (left y-axis) and µM (right y-axis) and plotted against time indicated in hours (x-axis); **b**) Body weight changes of K/BxN serum transferred mice treated i.p. every day for 14 days with high doses of serum albumin-antibody fusions (0.5 mL at 2 mg mL^{-1}, 1 mg per day per mice) normalized to starting weights. Serum albumin-antibody fusions SA129 (red), SA138 (blue) and controls SA^{CTR} (light gray) and PBS (white) do not elicit systemic toxicity as measured by weight loss. Treated mice gained weight and exhibited good body conditions. Weight was measured every other day and the indicated data represent the mean (dots) ± s.e.m. (bars) of five mice per group (n = 5); **c**) Schematic representation of the *in vivo* experimental prophylactic

setting design. Arthritogenic serum was injected on C57BL/6J twice, on days 0 and 2. Serum transferred K/BxN mice were treated i.p. daily, starting on day 0, with SA129, SA138 and SA^{CTR} fusions (0.5 mL at 2 mg mL^{-1}, 1 mg per day per mice); **d**) Schematic representation of the *in vivo* experimental therapeutic setting design. Arthritogenic serum was injected on C57BL/6J twice, on days 0 and 2. K/BxN serum transferred mice were treated i.p. daily, starting on day 4, with SA129, SA138 and SA^{CTR} fusions (0.5 mL at 2 mg mL^{-1}, 1 mg per day per mice). Arrows indicate days of injections. Ankles thickness and forelimbs of mice were measured every two days for a total of 14 days.

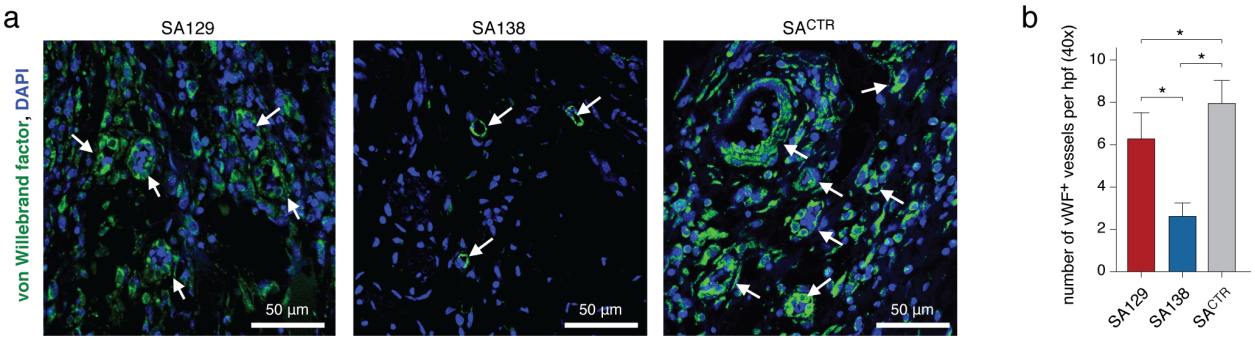

Supplementary Figure 12. Crossreactive serum albumin-antibody fusion prevents angiogenesis. Arthritogenic serum was injected into C57/BL6 on days 0 and 2. Mice were treated i.p. daily with SA129, SA138 and SA^{CTR} fusions (0.5 mL at 2 mg mL^{-1}, 1 mg per day per mice) beginning on day 0. **a**) Representative immunofluorescent staining of ankle tissue sections harvested on day 8 from mice treated with SA129, SA138 and control SA^{CTR}. Scale bar represents 50 µm. White arrows indicate von Willebrand factor-positive (vWF^{+}) vessels; **b**) Quantitation of vWF^{+} vessels per high-powered field (hpf) in the joint (n = 3 mice per condition). Statistical comparisons were made between each group using one-way analysis of variance (ANOVA), followed by Tukey's test to calculate P value: *$P < 0.05$.

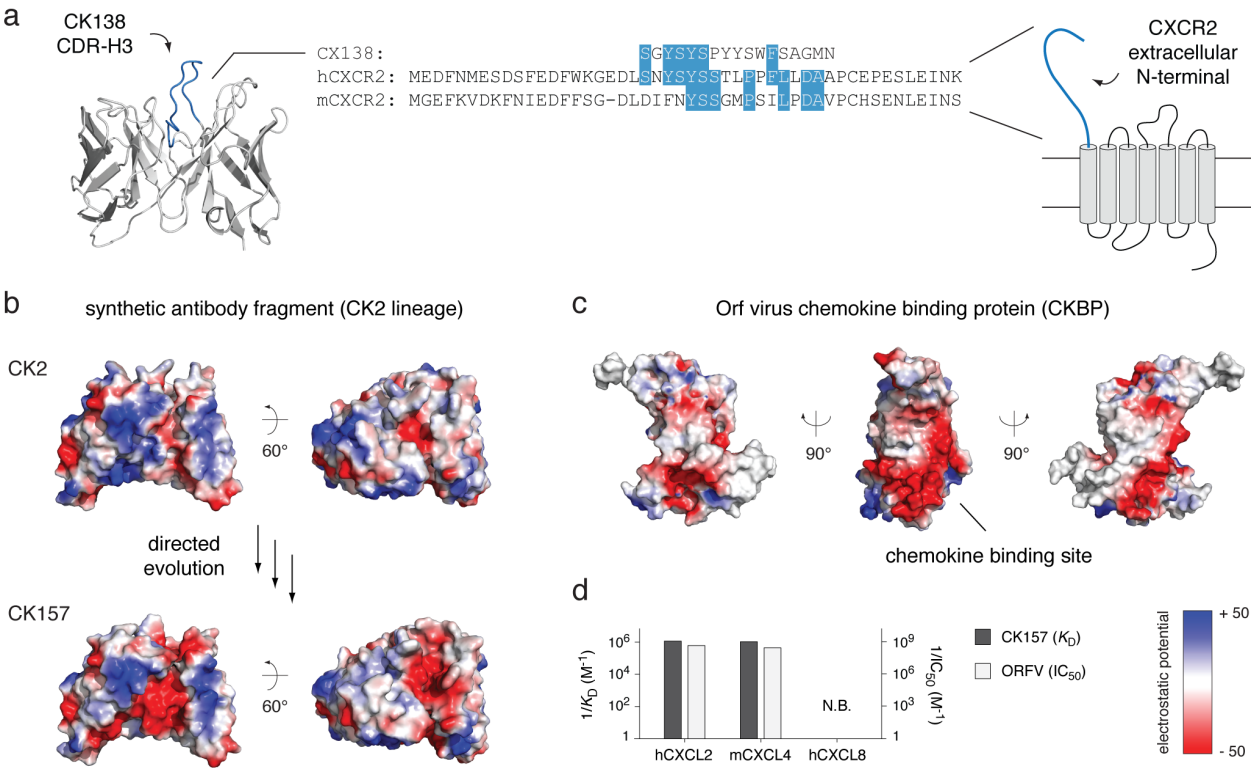

Supplementary Figure 13. Similarities with naturally occurring chemokine-binding proteins. a) The amino-acid composition and distribution of the CDR-H3 loop (blue) of the crossreactive CK138 antibody (left, represented as ribbons in light gray) resembles that of the N-terminus extracellular binding loop (blue) of CXCR2 receptor (right, schematically depicted)[21]. Sequence alignment of CDR-H3 loop and the N-terminus extracellular binding loop of both human ("h") and murine ("m") CXCR2 receptors are shown in the middles. Identical amino acid residues that are known to be important for the interaction with soluble ELR^+ CXC chemokine are shaded light blue; **b**) During the engineering process, the parental clone CK2 (top left) accumulated numerous surface exposed FWR mutations. These mutations caused the replacement of positive charged with negatively charged residues. The developed negative charged patches present on the surface of the evolved promiscuous antibody CK157 (bottom left) resembles that of the naturally evolved broad-spectrum viral chemokine binding proteins (vCKBP)[22-24]; **c**) Crystal structure of the promiscuous parapoxvirus orf virus (ORFV) CKBP protein (PDB ID: 4P5I)[22]. Similarly to the highly crossreactive CK157, the ORFV CKBP protein binds mCXCL2 (IC_{50} = 1 nM) and mCXCL4 (IC_{50} = 2.5 nM) but not hCXCL8. Functional studies have shown that ORFV CKBP exploits highly negatively charged groove and solvent

exposed hydrophobic amino acids to interact with both the CXCR2 and the GAG binding sites present on the surface of numerous ELR^+ CXC chemokines. Similarly to ORFV CKBP, CK157 antibody appears to recognize positively charged GAG binding residues present on the surface of ELR^+ CXC chemokines. Tridimensional structure models and electrostatic potential molecular surfaces of CK2, CK157 and ORFV CKBP proteins were generated and rendered using MODELLER and PyMOL, respectively. The structure of CK2 and CK157 are shown in two orientations (60° rotation) while the structure of ORFV CKBP is shown in three orientations (-90°, 0 and 90° rotation); **d**) Columns graph comparing the binding affinity (K_D) and the half maximal inhibitory concentration (IC_{50}) values measured for CK157 (dark gray) and ORFV CKBP (light gray) when tested against three CXC chemokines (mCXCL2, mCXCL4 and hCXCL8)[22], respectively. Data are presented as inverted of equilibrium binding constants ($1/K_D$; M^{-1}) and half maximal inhibitory concentrations ($1/IC_{50}$; M^{-1}).

Supplementary Tables

Chemokine nomenclature	
Systematic name	**Idiosyncratic name**
hCXCL1	GROα
hCXCL2	GROβ
hCXCL3	GROγ
hCXCL5	ENA-78
hCXCL6	GCP-2
hCXCL7	NAP-2
hCXCL8	IL-8
mCXCL1	KC
mCXCL2	MIP-2
mCXCL3	DCIP-1
mCXCL5	LIX
mCXCL7	NAP-2
hCXCL4	PF4
hCXCL9	MIG
hCXCL10	IP-10
hCXCL11	I-TAC
mCXCL4	PF4
mCXCL9	MIG
mCXCL10	IP-10
mCXCL11	I-TAC

Supplementary Table 1. The systematic names (left) of the chemokines are shown alongside their idiosyncratic nomenclature (right). “h” and “m” indicates human and murine, respectively.

	Binding affinities – K_D ± SE (nM)						
	hCXCL1	**hCXCL5**	**hCXCL8**	**mCXCL1**	**mCXCL2**	**mCXCL5**	**MBP**
CK1	> 2000	> 2000	> 2000	N.B.	N.B.	N.B.	N.B.
CK2	> 2000	605 ± 79	N.B.	481 ± 80	505 ± 86	> 2000	N.B.
CK3	N.B.	N.B.	N.B.	N.B.	N.B.	N.B.	N.B.
CK3*	562 ± 88	448 ± 73	410 ± 61	589 ± 75	445 ± 69	594 ± 81	522 ± 79
CK4	39.4 ± 7.4	> 2000	N.B.	744 ± 93	N.B.	> 2000	N.B.
CK5	> 2000	N.B.	> 2000	N.B.	N.B.	N.B.	N.B.
CK6	1675 ± 191	1987 ± 228	N.B.	N.B.	N.B.	N.B.	N.B.
CK7	N.B.	344 ± 68	N.B.	N.B.	N.B.	> 2000	N.B.
CK8	382 ± 73	N.B.	N.B.	825 ± 98	N.B.	N.B.	N.B.
CK9	N.B.	N.B.	N.B.	221 ± 49	278 ± 41	N.B.	N.B.
CK10	28.9 ± 4.5	N.B.	N.B.	801 ± 107	N.B.	N.B.	N.B.
CK11	425 ± 58	N.B.	N.B.	N.B.	N.B.	N.B.	N.B.
CK12	N.B.	N.B.	N.B.	N.B.	332 ± 57	N.B.	N.B.
CK13	N.B.	297 ± 98	N.B.	N.B.	N.B.	N.B.	N.B.
CK14	N.B.	N.B.	N.B.	N.B.	N.B.	269 ± 57	N.B.
CK15	N.B.	N.B.	N.B.	251 ± 25	N.B.	N.B.	N.B.
CK16	N.B.	102 ± 12	N.B.	N.B.	N.B.	N.B.	N.B.
CK17	N.B.	N.B.	N.B.	N.B.	N.B.	106 ± 11	N.B.
CK18	N.B.	N.B.	65 ± 6.1	N.B.	N.B.	N.B.	N.B.

Supplementary Table 2. Binding affinities of protein binders selected from a naïve library of synthetic single chain variable antibody fragments (scFv) displayed on the surface of yeast. Equilibrium binding constants (K_D) of each yeast-displayed antibody binder (CK) to three human (hCXCL1, hCXCL5 and hCXCL8) and three murine (mCXCL1, mCXCL2 and mCXCL5) ELR^+ CXC chemokine-SA fusion proteins (^{N}CXCL-SA^C) were determined by flow cytometry at 25 °C and physiological pH 7.4. Biotinylated maltose binding protein (MBP) bearing AviTag was used as control. The indicated values are means of at least three independent experiments. SE, standard error. N.B., not binding. Note: * stands for binding affinities measured using biotinylated ELR^+ CXC chemokines bearing AviTag at the C-terminus (^{N}CXCL-AviTag^C).

	Binding affinities – K_D ± SE (nM)					
	hCXCL1	**hCXCL5**	**hCXCL8**	**mCXCL1**	**mCXCL2**	**mCXCL5**
CK1	> 2000	> 2000	> 2000	N.B.	N.B.	N.B.
CK19	1262 ± 219	895 ± 72	212 ± 21	931 ± 81	> 2000	> 2000
CK21	> 2000	273 ± 17	144 ± 8.4	280 ± 37	> 2000	> 2000
CK23	> 2000	76.4 ± 5.8	104 ± 8.2	98.3 ± 33.4	> 2000	> 2000
CK63	> 2000	42.9 ± 8.2	15.2 ± 3.3	53.5 ± 9.8	> 2000	> 2000
CK66	594 ± 39	19.1 ± 1.6	21.5 ± 3.6	52.5 ± 8.1	> 2000	> 2000
CK72	120 ± 10	35.1 ± 2.3	25.8 ± 3.9	107 ± 15	63.6 ± 9.8	> 2000
CK138	61.9 ± 4.1	5.8 ± 0.9	7.4 ± 1.1	34.8 ± 3.2	36.2 ± 6.5	193 ± 22
CK140	64.6 ± 13	4.9 ± 0.6	8.2 ± 2.1	32.9 ± 2.8	33.2 ± 7.4	197 ± 10
CK2	> 2000	605 ± 79	N.B.	481 ± 80	505 ± 86	> 2000
CK41	304 ± 44	220 ± 65	N.B.	143 ± 14	75.4 ± 19	429 ± 24
CK43	368 ± 59	154 ± 31	N.B.	137 ± 11	213 ± 27	762 ± 98
CK108	110 ± 24	40.9 ± 6.4	N.B.	39.8 ± 7.5	40.6 ± 6.2	136 ± 19
CK111	62.9 ± 8.4	35.3 ± 2.1	N.B.	30.5 ± 2.8	23.8 ± 2.9	97.8 ± 11
CK119	56.7 ± 7.2	39.3 ± 6.4	N.B.	29.8 ± 2.1	27.5 ± 3.8	116 ± 20
CK152	48.4 ± 6.5	25.4 ± 2.8	N.B.	17.4 ± 2.8	21.6 ± 3.1	66.5 ± 10
CK155	24.1 ± 2.2	18.9 ± 2.5	N.B.	15.9 ± 2.4	33.5 ± 5.5	53.7 ± 8.9
CK157	36.2 ± 4.3	16.9 ± 1.7	N.B.	20.6 ± 4.1	18.2 ± 3.3	57.1 ± 3.9
CK4	39.4 ± 7.4	> 2000	N.B.	744 ± 93	N.B.	> 2000
CK50	3.1 ± 0.5	> 2000	N.B.	53.8 ± 3.5	> 2000	> 2000
CK56	12.6 ± 2.5	> 2000	N.B.	108 ± 4.5	> 2000	
CK125	1.23 ± 0.2	> 2000	N.B.	1.31 ± 0.1	> 2000	> 2000
CK129	0.79 ± 0.1	> 2000	N.B.	0.93 ± 0.1	> 2000	> 2000

Supplementary Table 3. Binding affinities of protein binders selected from the mutagenized libraries. Equilibrium binding constants (K_D) of each yeast-displayed antibody binder to human (hCXCL1, hCXCL5 and hCXCL8) and murine (mCXCL1, mCXCL2 and mCXCL5) ELR^+ CXC chemokines-SA fusion proteins (^{N}CXCL-SA^C) were determined by flow cytometry at 25 °C and

physiological pH 7.4. The indicated values are means of at least three independent experiments. SE, standard error. N.B., not binding.

Binding affinities – K_D ± SE (nM)				
	hCXCL1	**hCXCL5**	**mCXCL1**	**mCXCL2**
SA129	2.4 ± 0.4	N.B.	3.1 ± 0.7	N.B.
SA129ds1	1.9 ± 0.4	N.B.	2.5 ± 0.8	N.B.
SA129ds2	2.1 ± 0.5	N.B.	3.3 ± 0.7	N.B.
SA138	88 ± 11	N.B.	43 ± 3.8	N.B.
SA138ds1	2020 ± 102	N.B.	840 ± 52	N.B.
SA157	96.7 ± 8.4	126 ± 25	35.4 ± 4.1	29.1 ± 3.2
SA157-V_H	N.B.	N.B.	N.B.	N.B.
SA157-V_L	N.B.	N.B.	N.B.	N.B.
SA157-V_H + SA157-V_L	1540 ± 98	2214 ± 301	610 ± 74	553 ± 62

Supplementary Table 4. Binding affinities of variants of soluble crossreactive serum albumin-antibody fusions (SA129, SA138 and SA157) against human (hCXCL1 and hCXCL5) and murine (mCXCL1 and mCXCL2) ELR^+ CXC chemokine-SA fusion proteins (^{N}CXCL-SA^C). Equilibrium binding constants (K_D) were determined by flow cytometry at 25 °C and physiological pH 7.4. The indicated values are means of at least three independent experiments. SE, standard error. N.B., not binding.

Binding affinities – K_D ± SE (nM)						
	CK129 / SA129		**CK138 / SA138**		**CK157 / SA157***	
Display	**CK129**	**CXCL**	**CK138**	**CXCL**	**CK157**	**CXCL**
Soluble	**CXCL**	**SA129**	**CXCL**	**SA138**	**CXCL**	**SA157***
hCXCL1	1.0 ± 0.1	2.7 ± 0.3	41.5 ± 4.5	96.7 ± 2.4	61.1 ± 5.6	1433 ± 108
hCXCL2	13.9 ± 1.1	43.6 ± 4.1	267 ± 38	1591 ± 315	57.9 ± 4.8	853 ± 67
hCXCL3	5.7 ± 0.5	9.2 ± 0.9	349 ± 41	836 ± 130	53.9 ± 2.1	1034 ± 87
hCXCL5	> 2000	N.B.	5.8 ± 0.5	33.7 ± 2.2	26.3 ± 2.3	2125 ± 269
hCXCL6	N.B.	N.B.	153 ± 15	> 2000	46.6 ± 3.1	751 ± 88
hCXCL7	N.B.	N.B.	N.B.	40.6 ± 1.6	N.B.	N.B.
hCXCL8	N.B.	N.B.	6.9 ± 0.5	12.7 ± 0.9	N.B.	N.B.
mCXCL1	1.1 ± 0.1	2.9 ± 0.3	35.7 ± 3.3	29.4 ± 2.8	24.3 ± 1.9	666 ± 47
mCXCL2	> 2000	N.B.	29.1 ± 4.1	14.7 ± 0.5	19.9 ± 1.7	591 ± 62
mCXCL3	N.B.	N.B.	10.9 ± 1.1	31.4 ± 3.1	17.4 ± 1.4	2647 ± 264
mCXCL5	> 2000	N.B.	176 ± 21	357 ± 33	96.9 ± 6.9	2018 ± 169
mCXCL7	N.B.	N.B.	N.B.	N.B.	13.6 ± 0.8	528 ± 53
hCXCL4	N.B.	N.B.	167 ± 28	N.B.	112 ± 5.1	> 20000
hCXCL9	N.B.	N.B.	N.B.	N.B.	N.B.	N.B.
hCXCL10	N.B.	N.B.	N.B.	N.B.	45.5 ± 3.8	> 20000
hCXCL11	N.B.	N.B.	N.B.	N.B.	131 ± 11	> 20000
mCXCL4	N.B.	N.B.	N.B.	N.B.	17.1 ± 1.2	1770 ± 119
mCXCL9	N.B.	N.B.	N.B.	N.B.	N.B.	N.B.
mCXCL10	N.B.	N.B.	500 ± 55	N.B.	44.4 ± 3.7	N.B.
mCXCL11	N.B.	N.B.	N.B.	N.B.	124 ± 13	N.B.

Supplementary Table 5. Binding affinities of selected yeast display crossreactive protein binders against multiple human and murine CXC chemokines. Equilibrium binding constants (K_D) of both yeast-displayed crossreactive antibodies and CXC chemokine to twenty human and murine CXC chemokine-SA fusion proteins (^{N}CXCL-SA^{C}) and soluble SA129, SA138 and SA157*, respectively, were determined by flow cytometry at 25 °C and physiological pH 7.4. The indicated values are means of at least three independent experiments. SE, standard error. N.B., not binding. Note: * stands for SA157-V_L and SA157-V_H combined together equimolarly (SA157*).

Epitope mapping interactions					
	Ab275	**Ab276**	**SA129**	**SA138**	**SA157**
strong (0.0 – 0.25)	G17	L15	Q13	L12	N46
	T43	G17	L15	N46	
	N46	I18	I18	G47	
	G47	H19	N46	R48	
	R48	N46	G47		
	K49	K61	R48		
		K65			
moderate (0.25 – 0.5)	R8	Q16	T14	R8	I18
	L12	K21	G17	T14	H19
	T14	K45	G32	L15	K21
	L15	G47	T43	G32	K29
	Q16	K71	A50	A50	K45
	I18			L67	G47
	G32				I58
	K45				K65
	A50				K71
weak (0.5 – 0.75)	Q10	T14	N22	Q13	N22
	Q13	N22	K45	I18	
	N22	R48	E64	M66	
	N53	A50			
		I58			
		K60			
Total residues	19	18	14	13	11

Supplementary Table 6. Name and number of amino-acid residues identified during the hCXCL1 epitope mapping experiment. Mutations are grouped based on their ability to affect the binding of serum albumin-antibody fusions (SA129, SA138 and SA157) and antibodies (Ab275, Ab276) to hCXCL1 strongly (0.0 - 0.25), moderately (0.25 - 0.50) and weakly (0.50 - 0.75). Mutations that did not significantly affect the binding (0.75 - 1.0) are not reported.

Half maximal effective concentration – EC_{50} ± SE (nM)		
hCXCL1 / hCXCR2	**hCXCL8 / hCXCR2**	**hCXCL8 / hCXCR1**
24.7 ± 4.5	4.1 ± 0.4	4.9 ± 0.8

Supplementary Table 7. Fluorescence-based binding assay of wild type human CXCR1 and CXCR2 receptors to human ELR^+ CXC chemokines. HEK293 cells stably transfected with plasmids encoding human CXCR1 and CXCR2[25] were analyzed for their ligand binding properties with biotinylated hCXCL1 and hCXCL8. At the top of each table column is the name of the corresponding CXCR receptor tested. The half maximal effective concentration (EC_{50}) was determined by measuring the fluorescence-binding signal of cells encoding CXCR1 and CXCR2 receptors incubated with increasing concentrations of biotinylated ELR^+ CXC chemokines, ranging from 0.03 to 300 nM. The binding was determined by flow cytometry at 25 °C and physiological pH 7.4. The indicated values are means of at least three independent experiments. SE, standard error. N.B., not binding.

	Inhibitory activities – K_i ± SE (nM)		
	hCXCL1 / hCXCR2	**hCXCL8 / hCXCR2**	**hCXCL8 / hCXCR1**
SA129	1.54 ± 0.3	N.B.	N.B.
SA138	33.1 ± 6.5	6.53 ± 0.9	13.7 ± 1.9
SA157*	1420 ± 162	N.B.	N.B.
Ab	0.32 ± 0.08	0.24 ± 0.05	0.17 ± 0.02

Supplementary Table 8. Inhibitory activities of serum albumin-antibody fusions and commercial neutralizing antibodies towards human and murine ELR^+ CXC chemokines. The ability of serum albumin-antibody fusions SA129, SA138 and SA157* to compete for binding of biotinylated ELR^+ CXC chemokines (hCXCL1 and hCXCL8) to their cognate receptors CXCR1 and CXCR2 was determined by flow cytometry at 25 °C and physiological pH 7.4. Commercial neutralizing antibodies (Ab208 and Ab275) were included in the assay as positive control. Concentrations of biotinylated ELR^+ CXC chemokines that were equivalent to their EC_{50} values (hCXCL1 = 25 nM; hCXCL8 = 5 nM) were used for the experiments. The inhibition constants (K_i) were derived from the IC_{50} values using the Cheng-Prusoff equation. The indicated values are means of at least three independent experiments. SE, standard error. N.B., not binding.

Half maximal effective concentration – EC_{50} ± SE (nM)				
hCXCL1	**hCXCL5**	**hCXCL8**	**mCXCL1**	**mCXCL2**
0.94 ± 0.2	4.8 ± 0.8	1.29 ± 0.4	0.81 ± 0.9	2.5 ± 0.7

Supplementary Table 9. Flow cytometry-based free calcium mobilization assay of neutrophils in response to human and murine ELR^+ CXC chemokines. The half maximal effective concentration (EC_{50}) was determined by measuring the intracellular calcium level of human and murine neutrophils pre-loaded with ratiometric calcium indicator Indo-1 AM upon stimulation with increasing concentrations of five diverse ELR^+ CXC chemokines (hCXCL1, hCXCL5, hCXCL8, mCXCL1 and mCXCL2), ranging from 0.03 to 300 nM. The intracellular calcium levels were measured at 405/30 nm (Indo-1 low) and 485/nm (Indo-1 high) emission fluorescence after excitation at 355 nm. The indicated values are means of at least three independent experiments. SE, standard error. N.B., not binding.

	Inhibitory activities – K_i ± SE (nM)				
	hCXCL1	**hCXCL5**	**hCXCL8**	**mCXCL1**	**mCXCL2**
SA129	0.12 ± 0.02	> 2000	N.B.	0.33 ± 0.02	> 2000
SA138	44.9 ± 5.2	2.51 ± 0.5	1.62 ± 0.2	5.87 ± 0.6	3.2 ± 0.4
SA157*	334 ± 53	429 ± 61	N.B.	197 ± 29	145 ± 21
Ab	0.05 ± 0.006	1.20 ± 0.2	0.23 ± 0.03	0.08 ± 0.009	0.16 ± 0.03

Supplementary Table 10. Inhibitory activities of serum albumin-antibody fusions and commercial neutralizing antibodies towards human and murine ELR^+ CXC chemokines. The ability of promiscuous serum albumin-antibody fusions SA129, SA138 and SA157* to compete for binding of five diverse ELR^+ CXC chemokines (hCXCL1, hCXCL5, hCXCL8, mCXCL1 and mCXCL2) to their cognate receptors CXCR1 and CXCR2 expressed on the surface of human and murine neutrophils was determined by flow cytometry-based intracellular calcium mobilization assay. Commercial neutralizing antibodies (Ab208, Ab275, Ab452, Ab453 and Ab654) were included in the assay as positive control. Concentrations of ELR^+ CXC chemokines that were equivalent to their EC_{50} values (hCXCL1 = 1 nM; hCXCL5 = 5 nM; hCXCL8 = 1 nM; mCXCL1 = 7.5 nM and mCXCL2 = 2.5 nM) were used for the experiments. The inhibition constants (K_i) were derived from the IC_{50} values using the Cheng-Prusoff equation. The indicated values are means of at least three independent experiments. SE, standard error. N.B., not binding.

Pharmacokinetic parameters			
	SA129	**SA138**	**SA^{CTR}**
Dose (mg kg^{-1})	50	50	50
C_{max} (μg mL^{-1})	372.4	360.4	443.5
t_{max} (hr)	3	3	3
A	0.61	0.67	0.56
α (hr^{-1})	0.138	0.147	0.090
B	0.39	0.33	0.44
β (hr^{-1})	0.016	0.016	0.015
$t_{1/2,\alpha}$ (hr)	5.0	4.7	7.7
$t_{1/2,\beta}$ (hr)	43.5	42.4	47.4
$AUC_{0\text{-}tmax}$ (hr mg mL^{-1})	0.626	0.859	0.869
$AUC_{0\text{-}\infty}$ (μg day mL^{-1})	474.4	406.2	711.3
CL (mL day kg^{-1})	105.4	123.1	70.3
Number of mice	3	3	3

Supplementary Table 11. Pharmacokinetic parameters of serum albumin-antibody fusions SA129, SA138 and control (SA^{CTR}) administered as a single intraperitoneal (i.p.) dose. One milligram of each Alexa Fluor 647-labeled albumin fusion protein was injected i.p. (50 mg kg^{-1}) on C57BL/6 mice (n = 3 per construct) and their concentrations in blood plasma samples measured at various time points. *Dose*, amount of albumin fusion protein administered; C_{max}, maximal concentration (μg mL^{-1}) in plasma measured 3 hr after application; t_{max}, time (hr) to reach the C_{max}; $t_{1/2}$, elimination half-life, AUC, area under the curve; *CL*, clearance (mL day kg^{-1}); hr, hour. Serum levels were determined by a standard bi exponential decay equation[20].

Flow cytometry reagents for yeast surface display selection			
Primary	**Secondary**	**Primary**	**Secondary**
^{N}CXC^{C}-bio	Streptavidin 488	Chicken anti-c-myc	Goat anti-chicken 647
^{N}CXC^{C}-bio	Streptavidin 647	Chicken anti-c-myc	Goat anti-chicken 488
^{N}CXC^{C}-bio	Neutravidin 488	Chicken anti-c-myc	Goat anti-chicken 647
^{N}CXC^{C}-bio	Neutravidin 650	Chicken anti-c-myc	Goat anti-chicken 488
^{N}CXC^{C}-bio	Mouse anti-biotin VioBlue	Chicken anti-c-myc	Goat anti-chicken 647
^{N}CXC^{C}-bio	Mouse anti-biotin PE	Chicken anti-c-myc	Goat anti-chicken 647
^{N}CXC^{C}-bio	Mouse anti-biotin APC	Chicken anti-c-myc	Goat anti-chicken 488
^{N}CXC^{C}-bio	Streptavidin 488	Mouse anti-c-myc	Goat anti-mouse 647
^{N}CXC^{C}-bio	Streptavidin 647	Mouse anti-c-myc	Goat anti-mouse 488
^{N}CXC^{C}-bio	Neutravidin 488	Mouse anti-c-myc	Goat anti-mouse 647
^{N}CXC^{C}-bio	Neutravidin 650	Mouse anti-c-myc	Goat anti-mouse 488

Flow cytometry reagents for yeast surface display equilibrium binding titration			
Primary	**Secondary**	**Primary**	**Secondary**
^{N}CXC^{C}-bio	Streptavidin 647	Chicken anti-c-myc	Goat anti-chicken 488
^{N}CXC^{C}-bio	Streptavidin 647	Mouse anti-c-myc	Goat anti-mouse 488
^{N}CXC-SA^{C}	Mouse anti-His_6 tag 647	Chicken anti-c-myc	Goat anti-chicken 488

Antibodies	**Dilution**	**Company**
Mouse anti-biotin IgG-VioBlue (Bio3-18E7; 0.1 mg mL^{-1})	1:10	Miltenyi Biotec
Mouse anti-biotin IgG-APC (Bio3-18E7; 0.1 mg mL^{-1})	1:10	Miltenyi Biotec
Mouse anti-biotin IgG-PE (BK-1/39; 0.2 mg mL^{-1})	1:25	eBioscience
Neutravidin-DyLight 488 (1 mg mL^{-1})	1:100	Thermo Fisher Scientific
Neutravidin-DyLight 650 (1 mg mL^{-1})	1:100	Thermo Fisher Scientific
Streptavidin-Alexa Fluor 488 (2 mg mL^{-1})	1:250	Thermo Fisher Scientific
Streptavidin-Alexa Fluor 647 (2 mg mL^{-1})	1:250	Thermo Fisher Scientific
Chicken anti-c-myc IgY (1 mg mL^{-1})	1:500	Gallus Immunotech
Mouse anti-c-myc IgG (9E10; 0.7 mg mL^{-1})	1:500	Covance
Goat anti-chicken IgG-Alexa Fluor 647 (2 mg mL^{-1})	1:250	Thermo Fisher Scientific
Goat anti-chicken IgG-Alexa Fluor 488 (2 mg mL^{-1})	1:250	Thermo Fisher Scientific
Goat anti-mouse IgG-Alexa Fluor 488 (2 mg mL^{-1})	1:250	Thermo Fisher Scientific
Goat anti-mouse IgG-Alexa Fluor 647 (2 mg mL^{-1})	1:250	Thermo Fisher Scientific
Mouse anti-His tag IgG-Alexa Fluor 647 (0.2 mg mL^{-1})	1:50	Qiagen

Supplementary Table 12. Flow cytometry reagents used for yeast surface display selection and equilibrium binding titration. Combinations of detection reagents used for both primary and secondary staining are reported. Not listed biotinylated control proteins lysozyme (5 mg mL^{-1}) and MBP-AviTag fusion (1 mg mL^{-1}) were purchased from GeneTex and Avidity, respectively.

Commercial recombinant proteins and antibodies for binding assays on yeast and mammalian cells		
Antibodies	**Dilution**	**Company**
Mouse anti-human CD16 IgG-APC (3G8; 0.15 mg mL^{-1})	1:500	BioLegend
Mouse anti-human CD66b IgM-FITC antibody (G10F5; 0.3 mg mL^{-1})	1:500	BioLegend
Mouse anti-human CD45 IgG-PE (HI30; 0.01 mg mL^{-1})	1:50	BioLegend
Rat anti-mouse CD11b IgG-APC (M1/70; 0.2 mg mL^{-1})	1:500	BioLegend
Rat anti-mouse Ly-6G/Ly-6C (Gr-1) IgG-PE (RB6-8C5; 0.2 mg mL^{-1})	1:500	BioLegend
Mouse anti-human CXCR1 IgG-PE (8F1; 0.025 mg mL^{-1})	1:20	BioLegend
Mouse anti-human CXCR2 IgG-APC (5E8; 0.025 mg mL^{-1})	1:20	BioLegend

Antibodies	**Concentration**	**Company**
Mouse anti-hCXCL1 IgG_{2B} (clone 20326, MAB275)	0.5 mg mL^{-1}	R&D Systems
Mouse anti-hCXCL1 IgG_1 (clone 31716, MAB276)	0.5 mg mL^{-1}	R&D Systems
Mouse anti-hCXCL5 IgG_1 (clone 33170, MAB654)	0.5 mg mL^{-1}	R&D Systems
Mouse anti-hCXCL8 IgG_1 (clone 6217, MAB208)	0.5 mg mL^{-1}	R&D Systems
Rat anti-mCXCL1 IgG_{2A} (clone 48415, MAB453)	0.5 mg mL^{-1}	R&D Systems
Rat anti-mCXCL2 IgG_{2B} (clone 40605, MAB452)	0.5 mg mL^{-1}	R&D Systems
Mouse anti-hCXCL8 IgG_1 (clone E8N1)	0.5 mg mL^{-1}	BioLegend
Mouse anti-hCXCL8 IgG_1 (clone H8A5)	0.5 mg mL^{-1}	BioLegend

Recombinant proteins	**Concentration**	**Company**
hCXCL1 (275-GR-010)	100 µg mL^{-1}	R&D Systems
hCXCL5 (254-XB-025)	100 µg mL^{-1}	R&D Systems
hCXCL8 (208-IL-010)	100 µg mL^{-1}	R&D Systems
mCXCL1 (453-KC-010)	100 µg mL^{-1}	R&D Systems
mCXCL2 (452-M2-010)	100 µg mL^{-1}	R&D Systems
hCCL2-His Tag (10134-H08Y)	100 µg mL^{-1}	Sino Biological
rCCL5-His Tag (80038-R08Y)	100 µg mL^{-1}	Sino Biological
mCCL20-His Tag (50048-M08B)	100 µg mL^{-1}	Sino Biological
hCCL22-His Tag (10163-H07E)	100 µg mL^{-1}	Sino Biological
hCCL28-His Tag (10618-H07E)	100 µg mL^{-1}	Sino Biological
mC5a-His Tag (SRP4895A)	100 µg mL^{-1}	Sigma-Aldrich

Supplementary Table 13. Commercial recombinant proteins and antibodies used for yeast surface display equilibrium binding titration, epitope mapping, competitive flow cytometry-

based binding assay, neutrophil characterization and competitive flow cytometry-based intracellular calcium mobilization assay. Neutralizing antibodies targeting human and murine ELR^+ CXC chemokines were supplied as sterile solution in 1X PBS pH 7.4 (R&D Systems) or 1X PBS pH 7.2 containing 0.09% w/v NaN_3 in the presence or absence of 0.2% w/v BSA (BioLegend). Recombinant endotoxin-free human and murine ELR+ CXCL chemokines were purchased from R&D Systems. Recombinant CCL chemokines were purchased from Sino Biological. Recombinant complement component C5a was purchased from Sigma-Aldrich. All recombinant proteins were reconstituted in sterile 1X PBS pH 7.4 containing 0.1% w/v BSA to a final concentration of 100 μg mL^{-1}. Goat anti-mouse IgG-Alexa Fluor 647 (2 mg mL^{-1}) and goat anti-rat IgG-Alexa Fluor 647 (2 mg mL^{-1}) antibodies (Thermo Fisher Scientific) have been used as secondary reagents for the detection of mouse and rat monoclonal antibodies, respectively.

Supplementary References

1. Arevalo, J.H., Taussig, M.J. & Wilson, I.A. Molecular basis of crossreactivity and the limits of antibody-antigen complementarity. *Nature* **365**, 859-863 (1993).
2. James, L.C., Roversi, P. & Tawfik, D.S. Antibody multispecificity mediated by conformational diversity. *Science* **299**, 1362-1367 (2003).
3. James, L.C. & Tawfik, D.S. The specificity of cross-reactivity: promiscuous antibody binding involves specific hydrogen bonds rather than nonspecific hydrophobic stickiness. *Protein science : a publication of the Protein Society* **12**, 2183-2193 (2003).
4. Aharoni, A. et al. The 'evolvability' of promiscuous protein functions. *Nature genetics* **37**, 73-76 (2005).
5. James, L.C. & Tawfik, D.S. Conformational diversity and protein evolution--a 60-year-old hypothesis revisited. *Trends in biochemical sciences* **28**, 361-368 (2003).
6. Zimmermann, J. et al. Antibody evolution constrains conformational heterogeneity by tailoring protein dynamics. *Proc Natl Acad Sci U S A* **103**, 13722-13727 (2006).
7. MacArthur, M.W. & Thornton, J.M. Influence of proline residues on protein conformation. *J Mol Biol* **218**, 397-412 (1991).
8. Klein, F. et al. Somatic mutations of the immunoglobulin framework are generally required for broad and potent HIV-1 neutralization. *Cell* **153**, 126-138 (2013).
9. McFarland, B.J. & Strong, R.K. Thermodynamic analysis of degenerate recognition by the NKG2D immunoreceptor: not induced fit but rigid adaptation. *Immunity* **19**, 803-812 (2003).
10. McFarland, B.J., Kortemme, T., Yu, S.F., Baker, D. & Strong, R.K. Symmetry recognizing asymmetry: analysis of the interactions between the C-type lectin-like immunoreceptor NKG2D and MHC class I-like ligands. *Structure* **11**, 411-422 (2003).
11. Fields, B.A., Goldbaum, F.A., Ysern, X., Poljak, R.J. & Mariuzza, R.A. Molecular basis of antigen mimicry by an anti-idiotope. *Nature* **374**, 739-742 (1995).
12. Sethi, D.K., Agarwal, A., Manivel, V., Rao, K.V. & Salunke, D.M. Differential epitope positioning within the germline antibody paratope enhances promiscuity in the primary immune response. *Immunity* **24**, 429-438 (2006).
13. Wilkinson, I.C. et al. High resolution NMR-based model for the structure of a scFv-IL-1beta complex: potential for NMR as a key tool in therapeutic antibody design and development. *J Biol Chem* **284**, 31928-31935 (2009).
14. Reiter, Y. et al. Stabilization of the Fv fragments in recombinant immunotoxins by disulfide bonds engineered into conserved framework regions. *Biochemistry* **33**, 5451-5459 (1994).
15. Jung, S.H., Pastan, I. & Lee, B. Design of interchain disulfide bonds in the framework region of the Fv fragment of the monoclonal antibody B3. *Proteins* **19**, 35-47 (1994).
16. Weatherill, E.E. et al. Towards a universal disulphide stabilised single chain Fv format: importance of interchain disulphide bond location and vL-vH orientation. *Protein Eng Des Sel* **25**, 321-329 (2012).
17. Graff, C.P., Chester, K., Begent, R. & Wittrup, K.D. Directed evolution of an anti-carcinoembryonic antigen scFv with a 4-day monovalent dissociation half-time at 37 degrees C. *Protein Eng Des Sel* **17**, 293-304 (2004).

18. Fairbrother, W.J., Reilly, D., Colby, T.J., Hesselgesser, J. & Horuk, R. The solution structure of melanoma growth stimulating activity. *J Mol Biol* **242**, 252-270 (1994).
19. Ahmad, S., Gromiha, M., Fawareh, H. & Sarai, A. ASAView: database and tool for solvent accessibility representation in proteins. *BMC Bioinformatics* **5**, 51 (2004).
20. Kelly, R.L. et al. High throughput cross-interaction measures for human IgG1 antibodies correlate with clearance rates in mice. *MAbs* **7**, 770-777 (2015).
21. Prado, G.N. et al. Chemokine signaling specificity: essential role for the N-terminal domain of chemokine receptors. *Biochemistry* **46**, 8961-8968 (2007).
22. Counago, R.M. et al. Structures of Orf Virus Chemokine Binding Protein in Complex with Host Chemokines Reveal Clues to Broad Binding Specificity. *Structure* **23**, 1199-1213 (2015).
23. Ruiz-Arguello, M.B. et al. An ectromelia virus protein that interacts with chemokines through their glycosaminoglycan binding domain. *J Virol* **82**, 917-926 (2008).
24. Antonets, D.V., Nepomnyashchikh, T.S. & Shchelkunov, S.N. SECRET domain of variola virus CrmB protein can be a member of poxviral type II chemokine-binding proteins family. *BMC Res Notes* **3**, 271 (2010).
25. Ben-Baruch, A. et al. IL-8 and NAP-2 differ in their capacities to bind and chemoattract 293 cells transfected with either IL-8 receptor type A or type B. *Cytokine* **9**, 37-45 (1997).